
**EVAUATION OF PWSCC SUBCRITICAL CRACK GROWTH IN
COMPLEX GEOMETRIES USING ABAQUS XFEM**

Date:

October 19, 2020

Prepared in response to Task B3 in User Need Request NRR-2020-004, by:

L. T. Hill

Engineering Mechanics Corporation of Columbus

F.W. Brust

Engineering Mechanics Corporation of Columbus

S. Kalyanam

Engineering Mechanics Corporation of Columbus

NRC Project Manager:

Giovanni Facco

Materials Engineer

Component Integrity Branch

**Division of Engineering
Office of Nuclear Regulatory Research
U.S. Nuclear Regulatory Commission
Washington, DC 20555-0001**

DISCLAIMER

This report was prepared as an account of work sponsored by an agency of the U.S. Government. Neither the U.S. Government nor any agency thereof, nor any employee, makes any warranty, expressed or implied, or assumes any legal liability or responsibility for any third party's use, or the results of such use, of any information, apparatus, product, or process disclosed in this publication, or represents that its use by such third party complies with applicable law.

This report does not contain or imply legally binding requirements. Nor does this report establish or modify any regulatory guidance or positions of the U.S. Nuclear Regulatory Commission and is not binding on the Commission.

**DRAFT Final Report
On**

**Support for XFEM Component Integrity Analysis: Task 3
Evaluation of PWSCC Subcritical Crack Growth in Complex
Geometries using Abaqus XFEM**

**U.S. Nuclear Regulatory Commission
Prime Contract No.: NRC-HQ-25-14-E-0004
Task Order No. 31310019F0075
Emc² Project Number: 19-G121-01
*As a Subcontractor to NUMARK Associates, Inc.***

to

**U.S. Nuclear Regulatory Commission
Washington, D.C. 20555-0001**

by

L.T. Hill, F.W. Brust and S. Kalyanam



**Engineering Mechanics Corporation of Columbus
3518 Riverside Drive, Suite 202
Columbus, OH 43221
Phone/Fax (614) 459-3200/6800**

October 19, 2020

*As a Subcontractor to
NUMARK Associates, Inc.
1220 19th Street, NW, Suite 500
Washington, DC 20036*

EXECUTIVE SUMMARY

This report represents the third of four total tasks associated with the *Support for XFEM Component Integrity Analysis* program. The other reports are completed or undergoing final review at present. Task 1 (Literature Survey) provides a literature review of the eXtended Finite Element Method (XFEM) which summarizes the capabilities and limitations for current codes which have implemented XFEM based crack growth. The Task 2 report discusses the Abaqus XFEM implementation coupled with a simplified fatigue procedure which allowed exploration of optimum parameter definitions to provide the most appropriate solutions for constant amplitude fatigue and PWSCC (Primary Water Stress Corrosion Cracking) crack growth analyses. The Task 2 report explores five crack geometry cases, from simple two-dimensional constant amplitude fatigue cases to the V.C. Summer hot leg dissimilar metal weld (DMW) PWSCC analysis for three-dimensional axial PWSCC growth and leakage. This Task 3 report provides detailed solutions for XFEM based crack growth analyses on the V.C. Summer DMW and a generic control rod drive mechanism (CRDM) J-Groove weldment. The Task 3 report summarizes the best Abaqus based XFEM solution parameter definitions and compares the solutions to crack growth rate analysis results obtained in the past using other methods. This Task 3 report also identifies limitations in the analysis process and pitfalls possible. Task 4 provides a summary of solutions performed by the NRC and contractors, and other organizations that may be used in the future for further benchmarking. The benchmark solutions presented provide references along with other data necessary to perform XFEM based solutions and predicted results using other PWSCC growth methods for benchmark comparisons.

In the Task 2 report, the built-in Abaqus XFEM capability was shown to accurately model relatively simple planar crack growth PWSCC and constant amplitude fatigue applications when prescribed modeling recommendations were followed.

For Task 3, Abaqus XFEM analyses were performed to determine the applicability of these recommended modeling practices in complex geometries with planar crack growth relevant to the nuclear power industry. Specifically, the Abaqus XFEM crack propagation results were compared to traditional PWSCC crack growth analyses for the following geometries:

- Reactor Pressure Vessel (RPV) Outlet Nozzle to Hot Leg Pipe DMW Axial Surface Flaw
- RPV CRDM Uphill J-groove weld Axial Surface Flaw

Using the general XFEM modeling recommendations, the built-in Abaqus XFEM capability was shown to be capable of modeling planar crack growth for these relatively complex PWSCC applications in terms of crack growth rate and crack shape metrics.

After successful comparison of the strain energy release rate for the initial flaw size with a simplified published stress intensity factor solution, the V.C. Summer hot leg DMW (DWM) nozzle flaw was grown from the internal wetted surface to the outer diameter of the Inconel 182 weldment. In so doing, the final crack shape was found to qualitatively match with the post-mortem through-wall axial crack. Crack growth rates were found to be within 2% when compared to a natural crack growth flow method analysis. The natural crack growth analysis method, which is considered the current best practice, allows for linear elastic crack growth rates to be inferred from the stress intensity factor solution for a stationary, independent finite element run which is combined with a user-specified growth law. Using a controlling software package, crack dimensions are then updated, a new finite element model mesh is created, and the process is repeated until a final crack size is reached.

Similarly, for the hillside CRDM nozzle, the strain energy release rate was compared between the XFEM-estimated propagating crack strain energy release rate and a traditional focused mesh J-Integral contour integral extraction of the strain energy release rate for the initial flaw size. XFEM results were found to

be match within 10%. With this confidence, a PWSCC crack growth analysis was performed from this internal wetted surface of the weld to the triple point (tube-weld-head) which represents a pressure boundary breach. While using essentially the same linear elastic modeling assumptions associated with crack growth, the XFEM approach was found to be approximately 20% more conservative in terms of crack depth growth rate than the previously modeled assessment that used the finite element alternating method (FEAM).

To summarize, the XFEM assessments were found to be within 20% of crack growth rates and similar crack growth shapes when compared to the previously reported assessments using the natural crack growth approach method (DMW nozzle) and the FEAM method (CRDM nozzle). When the differences in modeling assumptions between the various approaches are considered, this is believed to be quite reasonable.

However, stability of complex XFEM crack growth models is an issue with the current release of Abaqus associated with the nodal level set calculation for the growing XFEM crack. In fact, 30-50% of the sensitivity runs completed in this study resulted in an Abaqus system error (code abort). As a result, the current built-in Abaqus XFEM capability should be viewed as a research tool rather than production tool.

This report documents the models, parameters studied, and other supporting evidence associated with providing these findings.

ACKNOWLEDGEMENTS

The authors gratefully acknowledges the helpful comments provided by the NRC staff during the preparation of this report. In particular, the extensive comments, edits, and contributions from the Office of Nuclear Reactor Regulation and the Component Integrity Branch are gratefully appreciated.

TABLE OF CONTENTS

Executive Summary	ii
Acknowledgements	iv
Table of Contents	v
1 Introduction.....	1
2 Complex Geometries Assessed.....	2
2.1 Nozzle-To-Pipe Dissimilar Metal Weld Axial Surface Crack	2
2.1.1 Introduction.....	2
2.1.2 Modeling Details.....	4
2.1.3 Benchmark using AFEA	6
2.1.4 Results.....	7
2.1.5 Summary	16
2.2 CRDM Uphill J-groove weld Axial Surface Flaw	16
2.2.1 Introduction.....	16
2.2.2 Modeling Details.....	20
2.2.3 Benchmark using FEAM	23
2.2.4 Results.....	25
2.2.5 Summary	36
3 Key Observations	37
3.1 Quality of Results.....	37
3.2 Stability of Solution.....	37
3.3 Computational Resources.....	38
4 Conclusions.....	39
References.....	40
Appendix A – Parameter and Unit Conversion Excel Tool	42

1 INTRODUCTION

The extended finite element method (XFEM) is a finite element analysis (FEA) method that allows for mesh-independent analysis of discontinuities and singularities and can be used to simulate crack growth in complex geometries in a simplified manner. This capability is available in several commercial FEA codes, including Abaqus [1], and is potentially a powerful tool for representing cracks and simulating crack growth in industry relevant models. In addition to its XFEM capabilities, Abaqus can simulate fatigue crack growth using a Paris Law type relationship. Furthermore, Abaqus is capable of modeling this fatigue behavior via a simplified analysis, where a multi-cycle fatigue process is modeled in a single static step. This approach allow other types of subcritical crack growth, like PWSCC, to be modeled.

In Task 2 of this project [2], the conditions and assumptions of the simplified fatigue function were used to define a relationship between the Abaqus Paris-like fatigue crack growth law and a general PWSCC crack growth rate equation. By taking advantage of both the XFEM and this simplified linear elastic fatigue approach in Abaqus, analyses were executed to determine those parameters that control the accuracy, repeatability of analysis results, and computational resources for this capability. Specifically, simple two- and three-dimensional models were evaluated in a systemic approach as highlighted by the activities listed below:

- Evaluation Parameters – The crack growth rate and crack shape were used as the fundamental evaluation criteria for the geometries evaluated with results compared to traditional finite element crack growth results or other acceptable analytical solutions.
- Geometries Studied – Four basic geometries were used to evaluate the capabilities with a focus on different crack front shapes (curved versus straight) and crack growth planes (straight planar versus curvilinear).
- Input Parameters Studied – In addition to mesh parameters (mesh size and mesh type), element formulation, fatigue procedure and crack growth parameters were studied. Overall, over forty analysis models were completed in this study.

It was found that even performing basic subcritical linear elastic crack growth analyses will be a challenge without significant benchmarking of results for a given problem class. With that stated, general modeling recommendations were provided for PWSCC and constant amplitude loading fatigue applications as summarized below:

- Software Version: Abaqus/Standard 2020 or later
- Minimum Mesh Refinement of XFEM Enriched Region in Key Structural Dimensions:
 - Thickness (crack growth depth direction) 50-elements
 - Width (crack growth length direction) Use Thickness mesh seed
 - Height (perpendicular to initial crack plane) 10-elements with Thickness mesh seed
- Mesh Type: Structured
- Element Formulation: Quad/Hex with Reduced Integration

The analysis parameters for calculating subcritical crack growth (growth tolerance and general solution controls) should be set to default values. However, with careful evaluation, non-default parameters could be utilized to obtain robust, accurate solutions within reasonable computational times.

In this Task 3 report, two complex geometries that are of importance to the nuclear power industry are analyzed. Section 2 provides background, overview of the XFEM modeling approach and results for the two problems. Section 3 summarizes the key observations and findings of the analyses. Finally, concluding remarks are provided in Section 4.

2 COMPLEX GEOMETRIES ASSESSED

Traditionally, nuclear reactor operation has been limited by materials' degradation issues. One such degradation issue is PWSCC in pressurized water reactor plants which is an intergranular cracking mechanism in which cracks form in susceptible materials under corrosive environmental and high tensile stress conditions. In fact, PWSCC is known to occur due to a combination of four factors: (i) tensile welding residual stress (WRS), (ii) water chemistry, (iii) a susceptible material, and (iv) high temperature (usually greater than 274 °C [18]). Over the past decades, PWSCC has been continuously reported in diverse major components and associated welds such as steam generator tubes, pressurizer instruments, and dissimilar metal welding regions of the CRDM head penetration nozzles and reactor vessel nozzle-to-piping weldments [3] [4].

Several analytical and numerical methods have been previously applied to evaluate the PWSCC crack growth in nuclear power plants by utilizing advanced finite element (FE) analysis techniques that simulate various aspects of crack progression.[8] [12] Despite these analytical advances, many difficulties remain in modeling crack growth phenomena. Therefore, with the potential of greater accuracy and efficiency in crack growth modeling, the extended finite element method (XFEM) was adopted in this study as the extension of arbitrary cracks is allowed using a simplified fatigue procedure that can effectively model PWSCC.

For this particular study, we examined two examples of axial flaws involving PWSCC in pressurized water reactors DMWs:

- RPV Outlet Nozzle to Hot Leg Pipe DMW
- RPV CRDM Uphill J-groove weld

For the benchmark problems listed above and all other potential PWSCC benchmarks that will be discussed in Task 4, the assessments have been limited to straight planar crack growth. This is in part due to the assumptions and implementations of the previous assessments when utilizing the natural crack growth and the FEAM and in part due to the actual PWSCC cracking observations of essentially planar crack growth. If curvilinear planar crack growth is expected or is observed within the analysis, additional Abaqus XFEM benchmarking will be warranted. While XFEM in theory should be able to handle curvilinear crack growth trajectories, Task 2 findings [2] indicated that cracking turning was impeded with the built-in Abaqus XFEM capability.

2.1 Nozzle-To-Pipe Dissimilar Metal Weld Axial Surface Crack

2.1.1 Introduction

An analysis was performed for the axial PWSCC flaw (see Figure 1) that was found in the RPV hot leg of the V.C. Summer plant. [5] The purpose of the original assessment was to examine the effect of the resultant WRS and their potential impact on PWSCC. This geometry was complicated by the fact that a field weld repair was performed but not fully documented. To explain further, when this repair was performed in the field, welding proceeded to approximately halfway through thickness when defects were seen near the inner diameter (ID) surface. This resulted in grounding out much of ID leaving a bridge about halfway through. Then, when the welding restarted, the weld sequence was not documented whether the ID was welded first followed by outer diameter (OD) (inside-out) or vice versa. The general consensus is that it was ID-to-OD. Further, from an assessment perspective, the inside-outside weld repair sequence results in faster PWSCC growth rates. As a result, for the current purposes, only the inside-outside weld repair was examined with the built-in Abaqus XFEM capability for

comparison with previously observed and natural crack growth advanced finite element analysis (AFEA) results. [6] AFEA method is discussed in detail in Section 2.1.3 of this report

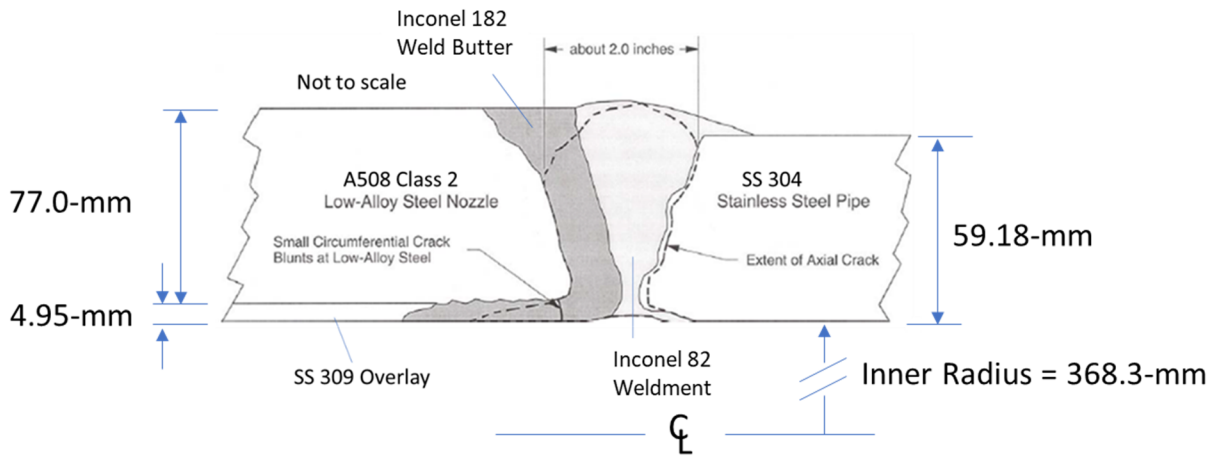


Figure 1 – Geometry and Observed V.C. Summer Hot Leg Axial Flaw in a Dissimilar Weld Metal Joint. Based on [6].

Using an axisymmetric FE model, the WRS in the vicinity of the hot leg to RPV nozzle bimetallic weld were obtained. The entire history of fabrication of the weld was included in the analysis, including the Inconel buttering, post-weld heat treatment (PWHT), weld deposition, weld grind-out and inside-out weld repair, hydro-testing, service temperature heat-up, and finally service loads. The results were then mapped onto a 360° FE model of the weld joint. Within the model as shown in Figure 2, a refined enrichment region, within a 5° segment, was defined such that a wetted surface semi-elliptical axial flaw could be propagated using XFEM in an Abaqus *FATIGUE procedure with PWSCC properties within the Alloy 182 weldment.

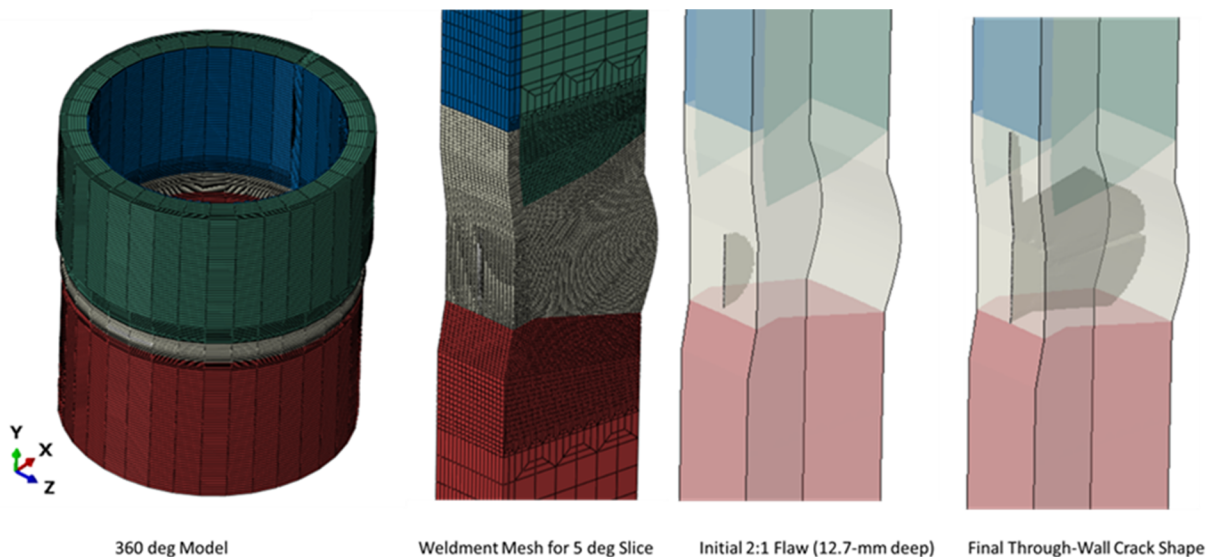


Figure 2 – V.C. Summer hot leg DMW 360° FE Mesh with Refined XFEM Enrichment Region

2.1.2 Modeling Details

Units: N-mm-hour-MPa

FEA Software: Abaqus 2020 (Build ID: 2019_09_13-12.49.31 163176)

Boundary Conditions: “Plane Sections Remain Plane” constraints were enforced at both ends of the piping via a cylindrically-oriented kinematic coupling which allowed radial dilation/contraction of the planes but constrain the other degrees of freedom.

Centered References Points control the motion for each constrained plane:

SS304 material Reference Node: $u_x=u_z=ur_x=ur_y=ur_z=0$ (y-translation free)

A508 Class 2 material Reference Node: $u_x=u_y=u_z=ur_x=ur_y=ur_z=0$ (fully fixed)

A tie constraint is applied to constrain the 355° coarse mesh to the 5° refinement mesh which contains the XFEM enrichment region.

Loading: The residual stress profile is mapped onto the 360° model via the use of the *MAP SOLUTION capability. Below, the primary driving force hoop stress is shown mapped onto the refined region which contains the XFEM enrichment region.

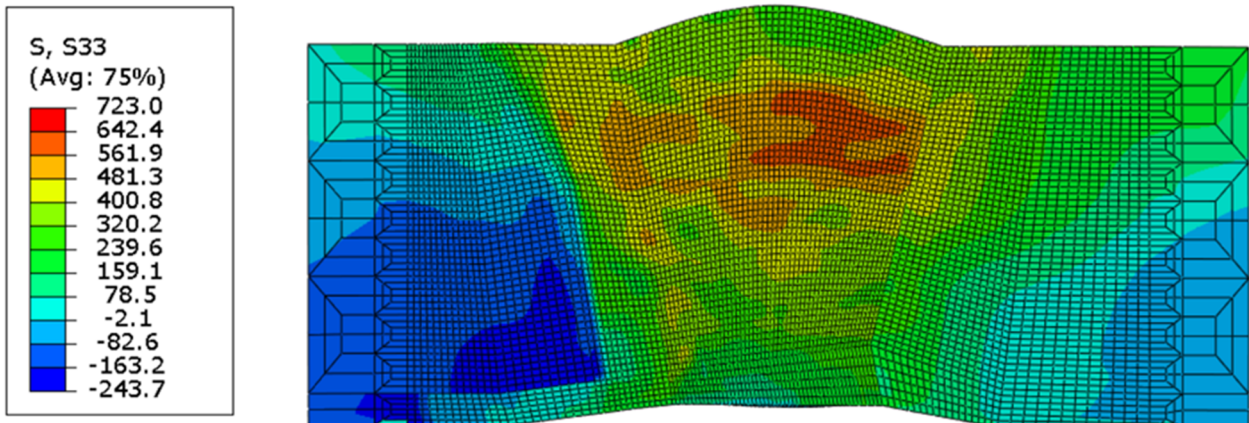


Figure 3 – V.C. Summer hot leg DWM FE Model Weld Residual Hoop Stress at 324 °C for an Uncracked Inconel 182 Weldment

The internal faces of the pipe, including the crack face, are exposed to an internal pressure of 15.513 MPa (2250 psig).

A corresponding end cap (thrust) loading of $P_y = 6734573.29$ N is applied to the A508 Class 2 material Reference Node due to the internal pressure loading. No piping loads were included in this assessment.

The hot leg assembly was set to a uniform temperature of 324 °C.

Material: Temperature-dependent Linear Elastic Material Properties were used at 324 °C for the Welded (SMA) Alloy 182, SS 309, SS 304 and A508 Class 2 materials. All relevant properties are defined and provided within the Supplemental Files Abaqus input files.

For the welded (SMA) Alloy 182 in pressurized water reactors (PWR) water conditions which is subject to the PWSCC mechanism, the MRP-115 [7] crack growth rate (75th percentile) for Alloy 182 was adopted in the present study at 324 °C.

$$\frac{da}{dt} = 2.0611 \cdot 10^{-3} K^{1.6}$$

when $\frac{da}{dt}$ is in in/year and K is in ksi $\sqrt{\text{in}}$ units.

Using the Appendix A Excel tool to convert between unit systems and parameters, the following equation was then used for the strain energy release rate crack growth relation in the required Abaqus format (see Task 2 [2] for more details):

$$\frac{da}{dt} = 4.0516 \cdot 10^{-4} G^{0.8}$$

when $\frac{da}{dt}$ is in mm/hour and G is in N/mm units.

It is appreciated that both Alloy 82 and 182 material exist in the weldment. As was stated in NUREG/CR-6954 [19], PWSCC crack growth rates in Alloy 182 are a factor of 2.6 higher than in Alloy 82; however, the rates along a direction transverse to the microstructural dendrites are a factor of two lower than those parallel to the dendrites. The effects of alloy type and crack orientation seem to cancel each other, yielding approximately the same growth rates for the weld and butter alloys. As a result, we have chosen to strictly model the weldment (including the butter) as Alloy 182. This is consistent with the assumption utilized in the AFEA benchmark analysis [6].

Analysis Steps:

As a precursor to the XFEM assessment, the axisymmetric welding residual model was provided followed by 360° model generation and results transfer. As these modeling details are of secondary importance for the XFEM assessment, only the necessary restart files are provided in the Supplemental Files. Then, with the use of the *MAP SOLUTION capability, the solution was mapped onto a new 360° 3-D model that contained a 5° slice refined section with the enriched region with a 2:1 initial XFEM flaw size (12.7-mm deep). Using the modified fatigue constants described in Task 2 [2], the *FATIGUE,TYPE=SIMPLIFIED was then used to grow the flaw due to the PWSCC mechanism.

The XFEM analysis is completed in two analysis steps:

- 1) *STATIC preload the structure to maximum value.
- 2) *FATIGUE, TYPE=SIMPLIFIED

Elements: C3D8R - 3D first-order 8-node continuum elements with reduced integration were used.

Meshes: A single highly refined structured mesh (1.0-mm x 1.0-mm in the plane of the crack) was utilized within the 5° mesh region that contains the enrichment zone and initial flaw. In the remaining of the model, a 5-mm x 5-mm in-plane mesh was used with 36 elements in the circumferential direction.

Parameters Studied:

In addition to the baseline assessment which incorporated the Task 2 general recommendations, independent analyses were used to evaluate subcritical fracture control and crack growth damage extrapolation tolerance controls influences on the run times, crack growth rates and shapes. The Abaqus CAE model database, input files, and other required files are provided in the Supplemental Materials file.

Table 1: Sensitivity Runs for V.C. Summer Hot Leg Axial Flaw in a Dissimilar Weld Metal Joint Assessment

VC Summer Hot Leg DWM Nozzle	Mesh Refinement	Element Formulation	Mesh Type	Crack Growth Position	Crack Growth ANGLEMAX	Fatigue Tolerance	Controls Disp Correction	Abaqus Input File Name
Baseline	Normal (60-elems)	Reduced	Structured	Default	-	0.1	0.01	VCsummer_ 101
Crack Growth Controls								
*FRACTURE CRITERION, POSITION=								
Default	N	R	S	Default	-	0.1	0.01	VCsummer_ 101
Nonlocal	N	R	S	Nonlocal	85	0.1	0.01	VCsummer_ 102
*FATIGUE tolerance								
0.1 (Default)	N	R	S	Default	-	0.1	0.01	VCsummer_ 101
0.175	N	R	S	Default	-	0.175	0.01	VCsummer_ 103
0.25	N	R	S	Default	-	0.25	0.01	VCsummer_ 104

2.1.3 Benchmark using AFEA

The V.C. Summer hot leg dissimilar metal v-groove weld axial crack evaluation was evaluated using the AFEA methodology following the work of Shim [6]. This benchmark was chosen as it contains both actual post-mortem flaw size measurements at this location and contains a numerical solution that uses the current best practice AFEA methodology for assessing PWSCC.

To introduce the method, the so called AFEA has been developed and used to model the ‘natural crack growth’ in simple geometries such as pipe components.[6] AFEA consists of calculating stress intensity factors at numerous points along the crack, growing the crack at each point, development of a new automatic FE mesh to produce the next crack size and shape, calculating the stress intensity factor along the crack front, and growing the crack further. The AFEA process requires an automated FE mesh generator and the entire process is managed with a controlling script (e.g. Python). The script develops a mesh for the current crack size, produces a FE model based input file, submits the FE job, extracts results (especially stress intensity factors along the crack front), grows the crack at points along the crack, develops next mesh, and so on until the crack reaches through thickness. This growth process typically requires tens of focused ‘spider’ crack meshes to be developed and often takes insignificant solution to model crack growth to through-wall. Because each solution is elastic, the solution time is manageable. The ability of AFEA to handle the elastic stress intensity factor that PWSCC is characterized by along with a mapped WRS as an elastic field was key in developing this for production-capable assessments.

In this effort a computer code, PipeFracCAE©, was employed to conduct the advanced finite element analyses. This computer code, using the commercial code Abaqus [2] as the solver, allows for planar arbitrary crack growth due to stress corrosion cracking. The natural development of the crack front is

controlled by the stress intensity factor of each crack tip location along the crack front. A semi-automated approach is used to incrementally control the growth of the arbitrary crack front. It is clearly noted that a contour integral evaluation in the AFEA method is used to extract the J-Integral. The J-Integral is widely accepted as a quasi-static fracture mechanics parameter for linear material response, with limitations, for nonlinear material response. For this linear elastic material problem, the J-Integral and strain energy release rate are equivalent.

In this benchmark, the axisymmetric WRS field described previously for the actual configuration was mapped onto a simplified 180-degree pipe with a uniform thickness and three distinct regions representing the A508C2 pipe, Alloy 182 weldment and SS 304 pipe. Seen in Figure 4, the initial 11.15-mm deep by 22.3 -mm long axial flaw was grown in eleven distinct time points to the 100% through-wall condition. The time to reach through-wall was estimated to be 1.18 years.

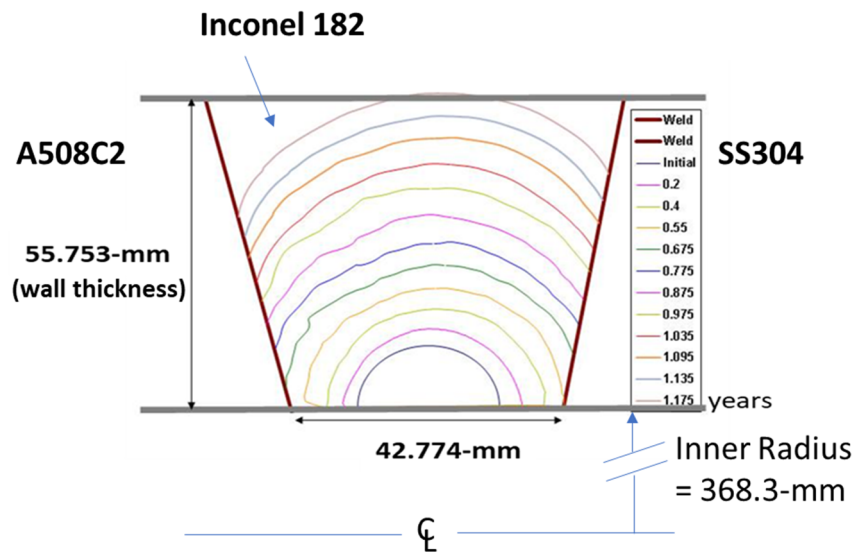


Figure 4 - Crack Shape Evolution as Function of Time for the AFEA of the PWSCC V.C. Summer Axial Surface Flaw in DWM Hot Leg

2.1.4 Results

2.1.4.1 Comparison of SIF Geometry Correction Factors Between Published Benchmark (API-579 [13]), AFEA Focused Crack Tip Mesh in Abaqus and Structured Meshes With XFEM Crack Propagation

To verify the general modeling recommendations in terms of crack driving force, a stress energy release rate sensitivity study was undertaken. Since the V.C. Summer hot leg DWM is a multi-material geometrically complex component, some simplifications were required. Fortunately, the API-579 [13] regulatory fitness-for-service code provides a standard weight-function based stress intensity factor (SIF) benchmark in Section 9B.5.10 for a semi-elliptical internal, surface flaw subjected to pressure in a straight pipe. For our needs, a one-hour time duration fatigue crack growth analysis for the V.C. Summer XFEM model was performed with the entire component being modeled as Inconel 182 and without the residual stress but still maintaining the internal pressure including the crack face pressure.

Table 2 summarizes the results as a function of position along the crack front for the initial flaw ($a/t=0.2$ with $2c/a=2$). This initial flaw size is consistent with the previous work performed by Shim [6]. To be clear, both the stationary crack XFEM technique and the AFEA technique use the contour integral to extract the J-Integral which is equivalent to the strain energy release rate for the linear elastic materials modeled. For propagating XFEM flaws in a simplified subcritical crack growth analysis (*FATIGUE,TYPE=SIMPLIFIED), a modified virtual crack-closure technique (VCCT) technique is used to directly extract G.

As can be seen, the XFEM ENRRTXFEM strain energy release rate output variable shows reasonable correlation (within 8% away from the surface) along the crack front when compared to the regulatory fitness-for-service benchmark. When the simplified subcritical crack growth procedure is changed to a static procedure such that the contour integral is used to evaluate a stationary crack, the strain energy release rates are also seen to be comparable. In addition, the initial flaw size was evaluated in a second-order, reduced integration model with a $1/r$ -singularity employed at the crack tip in a manner that is consistent with the AFEA solution (see Figure 5). Similar to the stationary crack XFEM contour integral model, strain energy release rates are seen to correlate well with the published benchmark and XFEM solutions.

It should be noted that strain energy release rates for the XFEM analyses do show oscillations along the semi-circular surface crack front. The oscillations arise at the location of the crack front and the edges of the FE, with the fluctuations being more pronounced where the crack front is farther away from being similar to the FE edges. Similar fluctuations were observed in other recent work [20,21]. To smooth the data, the XFEM strain energy release rates for three elements nearest the crack front angle are averaged and are listed in Tables 2 and 3. While the overall smoothing is good, one will note in Table 2 that the VCSummer_202 (propagating XFEM) run still sees some level of deviation from the other solutions near the 180 deg free surface.

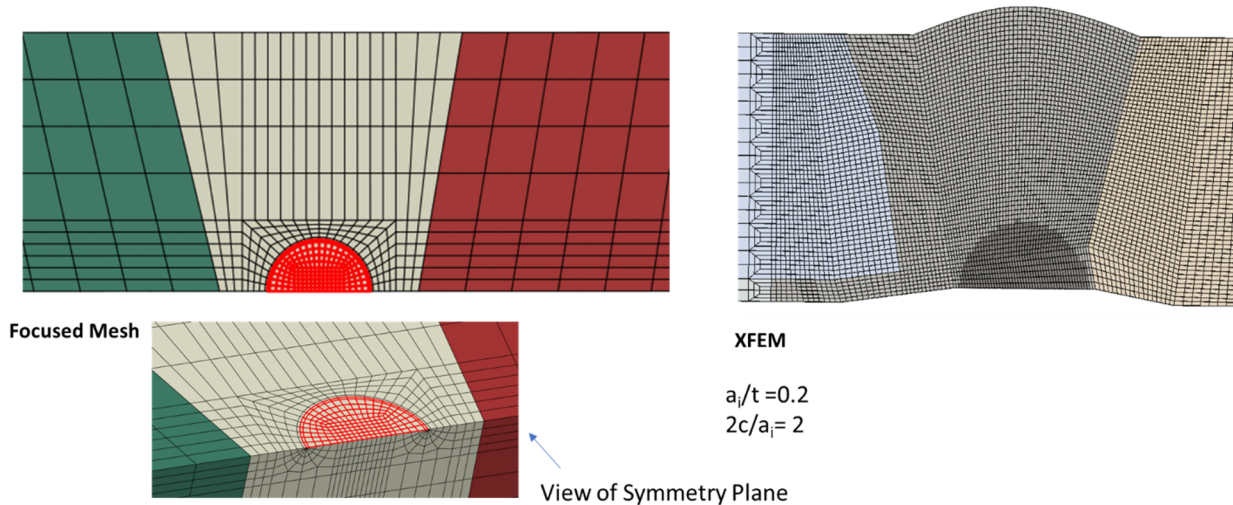
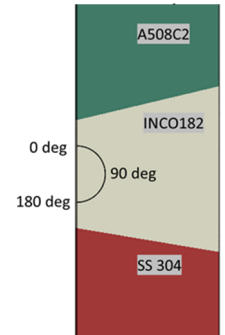


Figure 5 Focused and XFEM FE Model Meshes for Strain Energy Release Rate Calculations of the V.C. Summer Initial Internal Axial Surface Flaw ($a/t=0.2$, $2c/a= 2$) in hot leg DMW

Table 2 : Comparison of Strain Energy Release Rate (units: N/mm) for an internal axial elliptical flaw ($2c/2=2$, $a/t=0.2$) utilizing a Published Benchmark[13] along with Stationary and Propagating Crack Extraction Techniques in Abaqus with Pressure Loading Only (Three-element Average for XFEM Results at a Given Location)

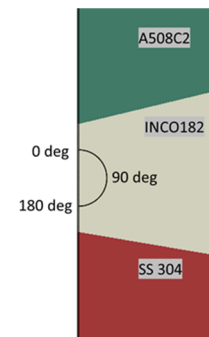
Analysis Run:	VCSummer_	202	203	201
Crack Front Angle (deg)	Published Benchmark API-579	XFEM		AFEA
	Straight Pipe Pressure Only INCO only	Propagating Modified VCCT VCSummer Pressure Only INCO only	Stationary Contour Integral VCSummer Pressure Only INCO only	Stationary Contour Integral Straight Pipe Pressure Only INCO only
0	1.456	1.382	1.317	1.308
45		1.125	1.068	1.067
90	1.064	0.976	0.995	1.062
135		1.103	1.084	1.104
180	1.456	1.025	1.349	1.307



To continue the calculated driving force work in a generalized sense, the inclusion of the different materials as opposed to just a single material (Inconel 182) and the inclusion of WRS values are tabulated as seen in Table 3. With the influence of single versus multi-material differences being minimal, the WRSes are seen to be the dominant load at smaller crack sizes.

Table 3: Comparison of Strain Energy Release Rate for an internal axial elliptical flaw ($2c/a=2$, $a/t=0.2$) in the VC Summer DWM Surge Nozzle illustrating influence of Weld Residua Stress (Three-element Average for XFEM Results at a Given Location)

Analysis Run:	202	204	101
Crack Front Angle (deg)	XFEM		
	Propagating Modified VCCT VCSummer Pressure Only INCO only	Propagating Modified VCCT VCSummer Pressure Only 4-material	Propagating Modified VCCT VCSummer WRS+Press 4-material
0	1.382	1.493	4.350
45	1.125	1.394	5.570
90	0.976	1.149	6.900
135	1.103	1.208	7.090
180	1.025	1.193	6.000



To summarize, acceptable crack driving force correlation (G values within ~8%) is seen between a published benchmark (API-579 [13]), AFEA-type focused crack tip mesh in Abaqus and structured meshes with XFEM crack propagation. Further, the WRS have been confirmed to be the dominant loading for smaller crack sizes.

2.1.4.2 Results Compared to AFEA and Post-Mortem Crack Shape from Actual Defect

Figure 6 shows the crack shape evolution as a function of time for the PWSCC VC Summer axial surface flaw in the hot leg DMW XFEM assessment. As expected, the shape of the XFEM crack growth was driven by the hoop WRS. This is seen in the figure as the early-stage crack growth at a given time is in the depth direction vs the in-plane length. Further, the location of the actual wall penetration (Figure 7) coincides with the high stress location of the XFEM predicted results.

Also, in Figure 7, results from the linear elastic natural crack growth (AFEA) analysis are shown overlaid on the final XFEM results. Figure 8 shows the crack depth at the deepest location as a function of time. The AFEA approach shows the time to reach through-wall is 1.18 years while the baseline XFEM analysis is 1.20 years. Of course, there are differences between the two approaches. This includes geometrical differences where XFEM uses the actual non-uniform thickness piping along with a crown on the weldment whereas the AFEA solution uses a straight pipe. Furthermore, while the initial flaw depth ratio (a/t) of 0.2 was used for both assessments, the actual depth value of 12.7-mm is used for the XFEM model and 11.15-mm is used for the AFEA. Also, the XFEM initial flaw was located centered in the Inconel 182 weldment while the AFEA assumed the center of the combed distance of the Inconel 182 weld with the butter layer. Other numerical differences exist such as the crack driving force extraction procedure (modified VCCT for the propagating XFEM analysis versus the contour integral extraction for instantaneous AFEA analysis). Despite the differences in the approaches, the overall comparison is seen to be quite good.

Still, there is some level of concern with the XFEM simulations associated with slight out-of-plane crack path oscillations. Figure 9 demonstrates the observed slight out-of-plane oscillations which occurred primarily, but not exclusively, at the edge of the enriched regions. As indicated in this figure, Abaqus is seen to abort at 99% of the through-wall thickness for the baseline analysis (VCSummer_101) at an element near the edge of the Alloy 182 enriched region. As noted in the figure, some of the other sensitivity analyses also encountered premature failure of the analysis.

In terms of the code abort issue, Abaqus reports the nodal level set values might not be correct at the location shown followed by the code abort. The provided level set in the code abort message is essentially perpendicular to the existing crack plane. There does not appear to be a systematic modeling parameter that consistently precludes this from occurring. Seen in Figure 9, the location is predominately but not exclusively along the crack front adjacent to the enriched region boundary. Further, there appears to some amount of crack path oscillatory behavior even in analysis cases that run to completion; however, more pronounced oscillations are seen to more likely result in code aborts. Finally, at no time prior to the code abort are any Newton-Raphson convergence problems noted in the solution. For the current Abaqus capability, the modeling recommendations defined in Task 2 and summarized in the Introduction remain the most stable parameters to provide accurate solutions.

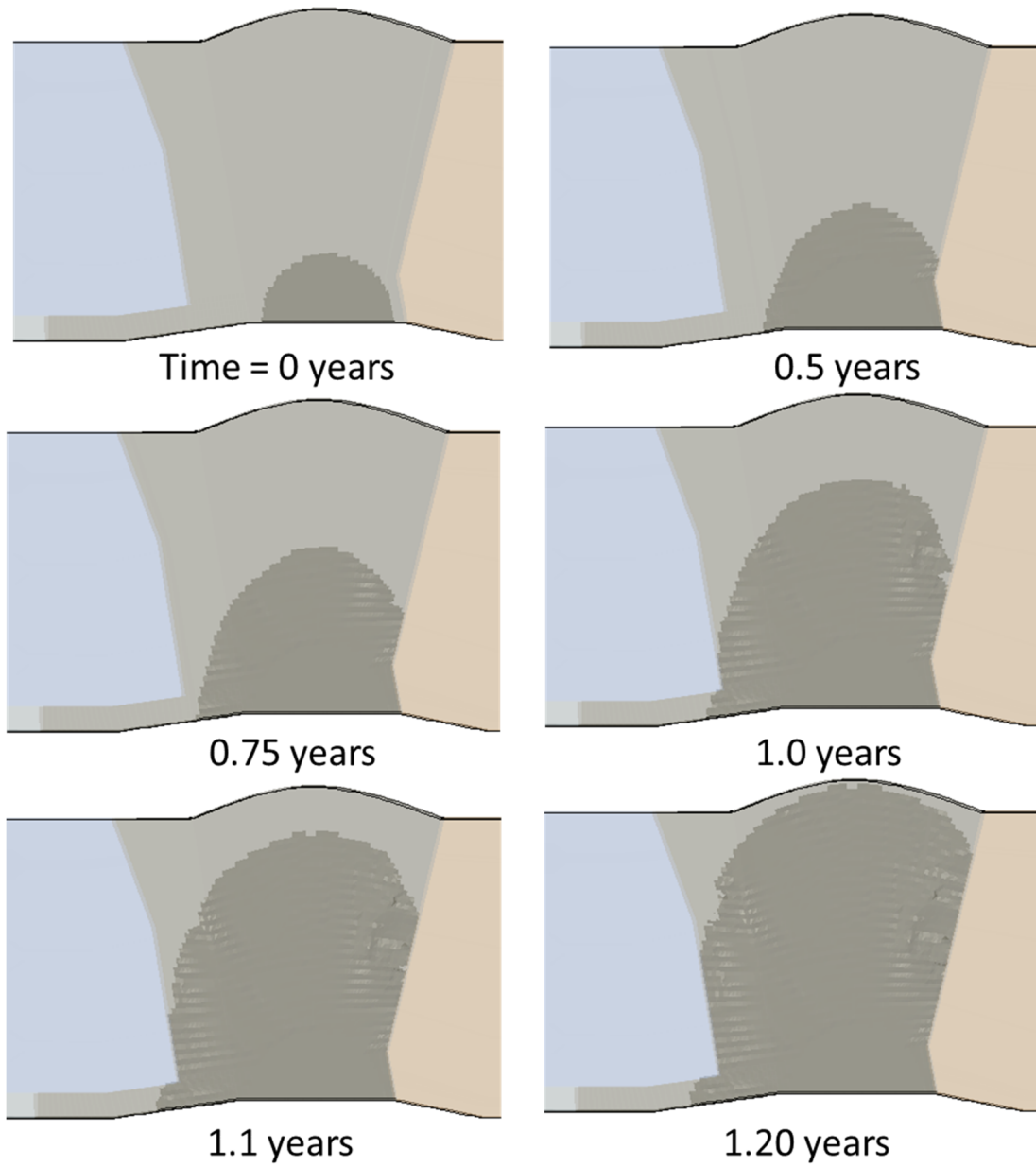


Figure 6 - Crack Shape Evolution as Function of Time for Baseline PWSCC V.C. Summer Axial Surface Flaw in DWM Hot Leg XFEM assessment

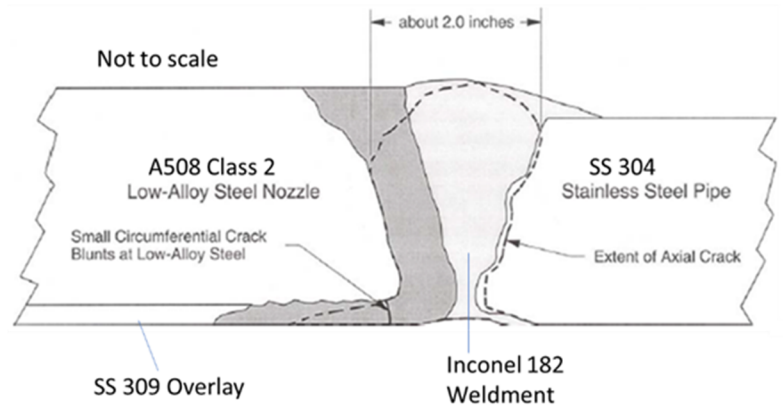
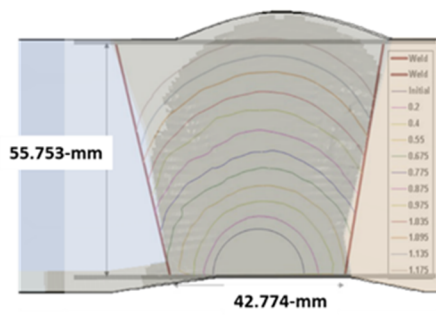


Figure 7 - Overlay of Natural Crack (Advanced FEA approach) Shape on the Baseline XFEM assessment along with Post-Mortem Crack Shape for PWSCC V.C. Summer Axial Surface Flaw in V.C. Summer hot leg DMW [6]

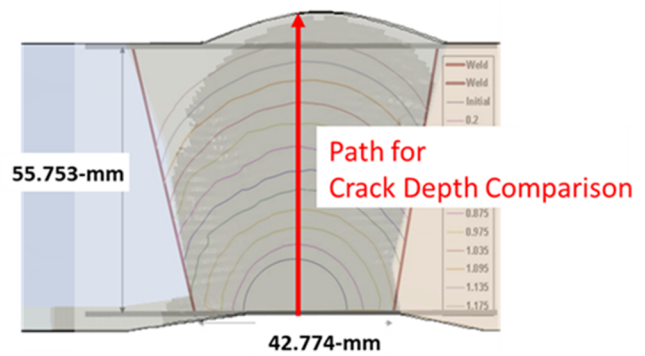
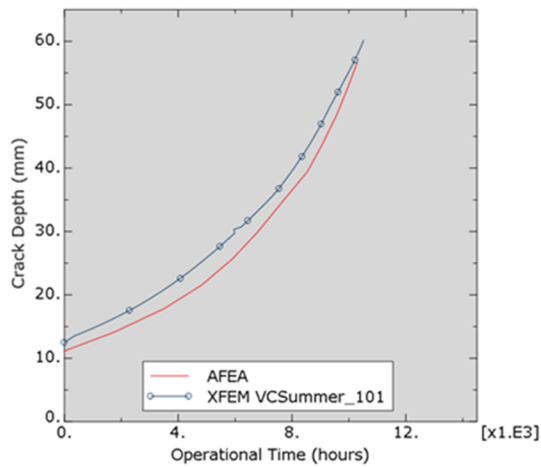


Figure 8 - Comparison of Crack Growth at Deepest Point as a Function of Time between AFEA and XFEM for PWSCC Axial Surface Crack in V.C. Summer hot leg DMW

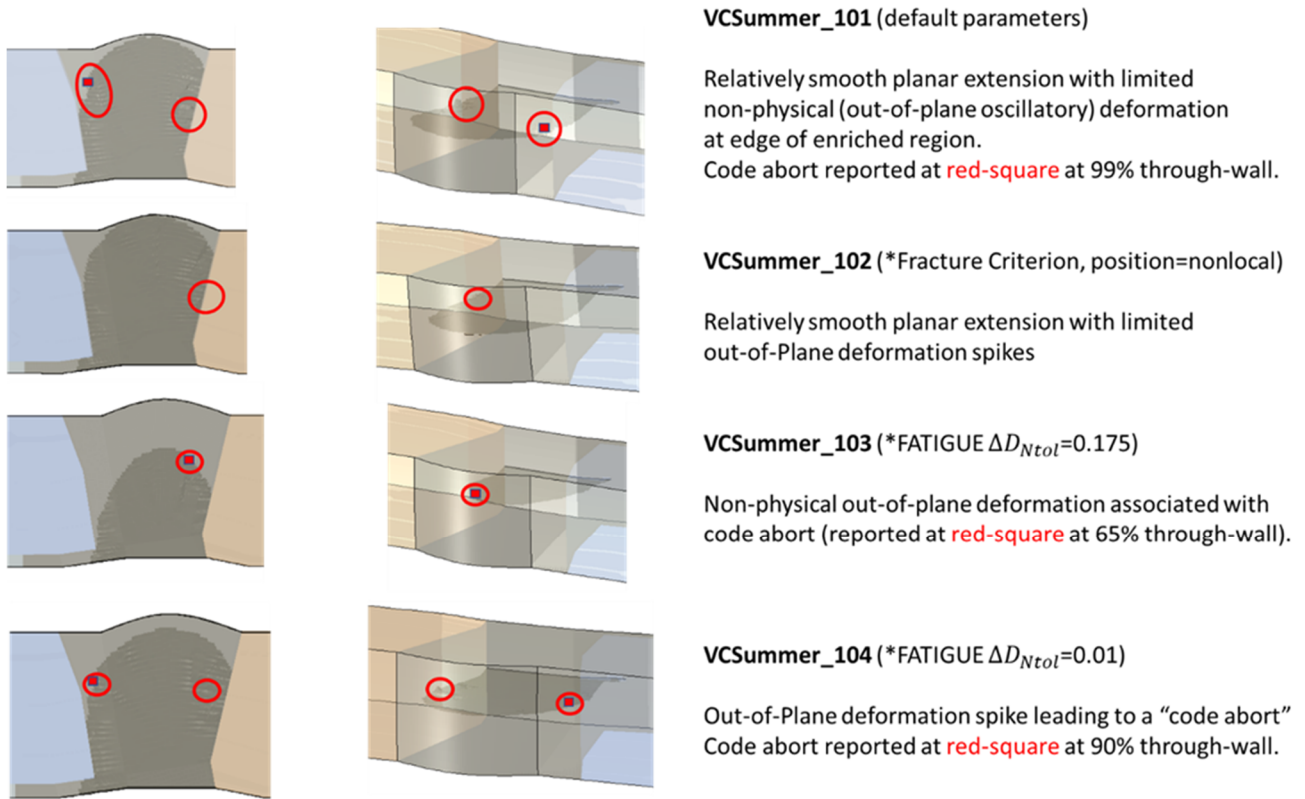


Figure 9 - Observed Out-of-Plane Crack Oscillations for PWSCC Axial Surface Crack in V.C. Summer hot leg DMW XFEM Assessments

2.1.4.3 Local Element Fracture Criterion: Default Versus POSITION=Nonlocal

In attempt to maintain a smooth, continuous three-dimensional crack front, the nonlocal averaging on the fracture criterion was studied. However, minimal changes were observed in the crack shape (Figure 9) and crack growth rate (Figure 10) for this near planar crack extension problem.

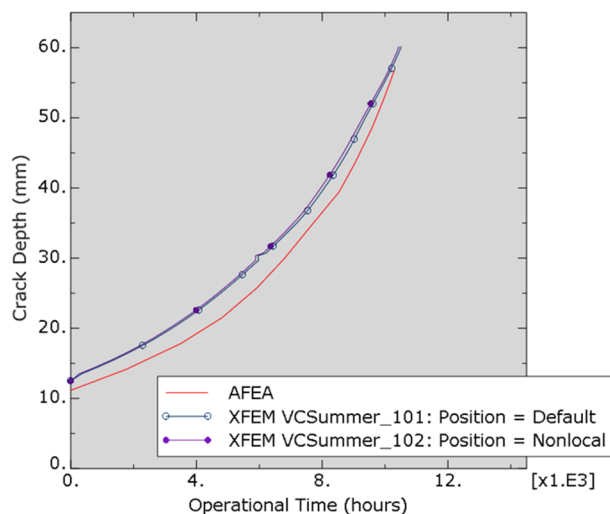


Figure 10 - Influence of Crack Growth POSITION Parameter on Crack Growth at Deepest Point as a Function of Time for PWSCC Axial Surface Crack in V.C. Summer hot leg DMW

2.1.4.4 Subcritical Damage Extrapolation Tolerance Parameter

For longer running analyses, the damage extrapolation tolerance parameter, ΔD_{Ntol} , can be used to accelerate the subcritical crack growth analysis and to provide a smooth solution for the crack front. Figure 11 shows that increasing ΔD_{Ntol} to 0.175 from the default of 0.1 does increase the crack growth rate while crack shapes at the same crack depth are seen to be deviated significantly from the baseline XFEM analysis. Further, when ΔD_{Ntol} is set to 0.175, a code abort is observed at an out-of-plane oscillatory (numerical artifact) deformation near the edge of the enrichment region at approximately the 60% of through-wall crack depth. When ΔD_{Ntol} is set to a tight value of 0.01, minimal changes are noted with the baseline analysis in terms of crack growth rate and crack shape.

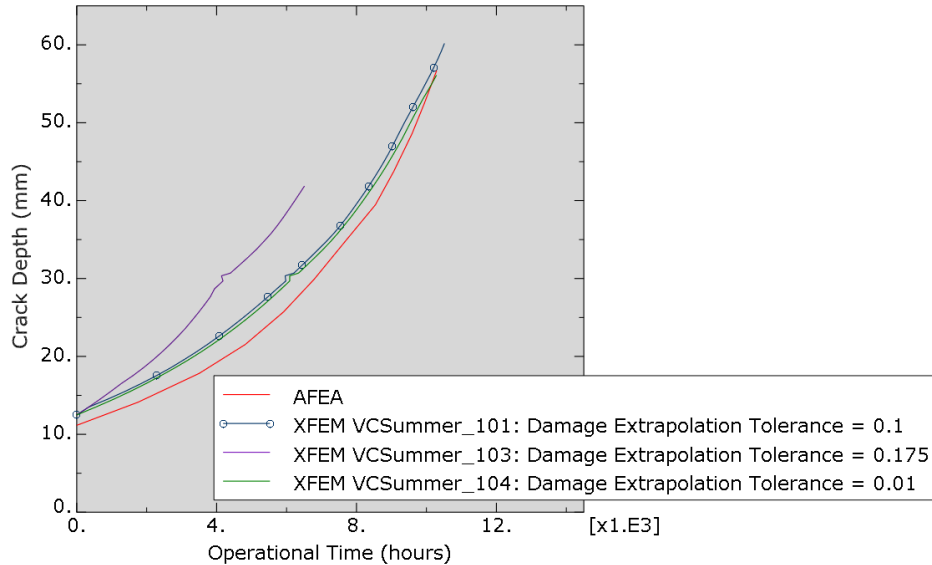


Figure 11 - Influence of Crack Growth Damage Extrapolation Tolerance Parameter on Crack Growth at Deepest Point as a Function of Time for PWSCC Axial Surface Crack in V.C. Summer hot leg DMW

2.1.4.5 Importance of Mesh Seed Size in Structural Height Direction

As was defined in the Task 2 report [2], the enriched region structural height (hoop-direction) region mesh seed was investigated using the recommended 1-mm mesh seed (baseline) and a coarse 2-mm mesh seed. Figure 12 shows the importance of maintaining the recommended mesh refinement in the structural height direction as the time to reach through-wall is predicted to increase by over 30% with the coarse mesh seed. Unlike the stationary crack contour integral (J-Integral) and interaction integral (SIF, K) where fairly coarse meshes are able to capture path independent driving force values, the propagating crack values are calculated for each crack front element with the linear elastic strain energy release rate, G, directly using the modified VCCT method. Hence, a nearly perfect cube shape is required as provided in the recommended meshing parameters.

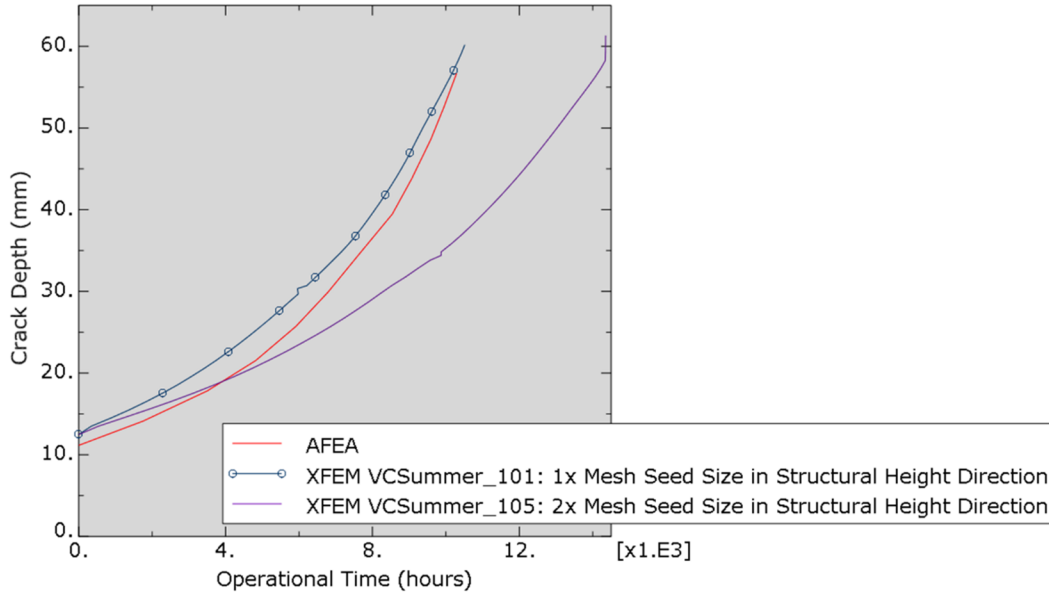


Figure 12 - Influence of Mesh Seed Size in Structural Height Direction on Crack Growth at Deepest Point as a Function of Time for PWSCC Axial Surface Crack in V.C. Summer hot leg DMW

2.1.4.6 Computational Cost

In terms of computational cost, Table 4 shows the XFEM capability is computationally viable. With the current Abaqus XFEM implementation, it is possible to achieve analysis runs in under one-day by utilizing multi-core simulations. Further, by increasing the ΔD_{Ntol} to increased values (e.g. 0.175 or 0.25), the runtimes can be reduced by approximately 2x while ensuring that a more conservative crack growth rate is obtained. This may be of benefit when a rough estimate, but not necessarily the most accurate, solution is required. However, it was seen in the final set of runs for the V.C. Summer analysis, that premature failure of the Abaqus simulation due to an internal code error did occur when the ΔD_{Ntol} was set to 0.175. As shown in Figure 9, Abaqus reported the nodal level set values might not be correct at the location shown followed by the crash. The provided level set is essentially perpendicular to the existing crack plane. There does not appear to be a systematic modeling parameter that consistently precludes this from occurring.

Table 4 – Computational Resources for the PWSCC V.C. Summer Axial Surface Flaw in DWM Hot Leg XFEM for Different Crack Extension Parameters

	VC_Summer	
	101	102
	Default	Nonlocal
Analysis Run:	101	102
Position:	Default	Nonlocal
Damage Extrapolation Tolerance:	0.1	0.1
Computer Wallclock Time* (hrs)	19.15	19.58
Increments	4415	4531
Iterations	4415	4531

* All computer runs were made with 10-cores with an Intel® Xeon® Gold 6148 2.4GHz chip on RHEL 7.5

In relation to other numerical techniques, such as the linear elastic natural crack growth approach, those solutions will be faster from a processor time perspective (on the order of a dozen solver passes).

However, unless proper scripting algorithms exist, the setup time will likely reduce the total analysis time advantage.

2.1.5 Summary

- Using the general XFEM modeling recommendations, the built-in Abaqus XFEM capability has shown to be robust for modeling a relatively complex model PWSCC application. The final through-wall crack shape was found to be similar to the observed V.C. Summer crack.
- While using essentially the same linear elastic modeling assumptions associated with crack growth, the XFEM approach was found to be slightly more conservative than AFEA. Among the differences listed, this is believed to primarily be due to the subcritical damage extrapolation tolerance parameter.
- Up to 50% of the cases studied, code aborts have occurred in Abaqus sensitivity analysis runs, occurring primarily when the Alloy 182 crack extended to the boundary region adjacent to the stainless steel and steel. Time-critical analyses could be compromised until this issue is resolved.

2.2 CRDM Uphill J-groove weld Axial Surface Flaw

2.2.1 Introduction

This section addresses the assessment of PWSCC cracking in CRDMs in nuclear RPV heads. In PWRs, the RPV head contains numerous penetration nozzles so that CRDMs can be inserted to allow control rods to be articulated as needed for reactor operation. Shown in Figure 13, the nozzle consists of an Alloy 600 pipe (or tube) that goes through the head has a partial penetration weld to the vessel at the ID surface of the head. This weld is referred to as the J-groove Weld. The weld material at the time of the 1970s era construction was Alloy 82/182. Alloy 600 and Alloy 82/182 were originally chosen for their excellent general corrosion resistance and due to the fact that the coefficient of thermal expansion closely matches that of the RPV head low-alloy steel (SA 508 Class 3). For this study, the nozzle tube has a 101.6-mm outside diameter with a wall thickness of 15.875-mm [8].

Here, we consider growth of axial crack emanating from the wetted side of the weldment through the weld and tube up to the triple point which may result in a leak. When a crack reaches the triple point, corrosion of the ferritic nozzle material may occur. In addition, if the axial crack penetrates the weld to the triple point it may turn to become a circumferential crack starting on the tube OD. If this circumferential crack were to grow to be a long circumferential crack before breaking to the tube ID, it is possible that the tube can eject causing a safety concern.

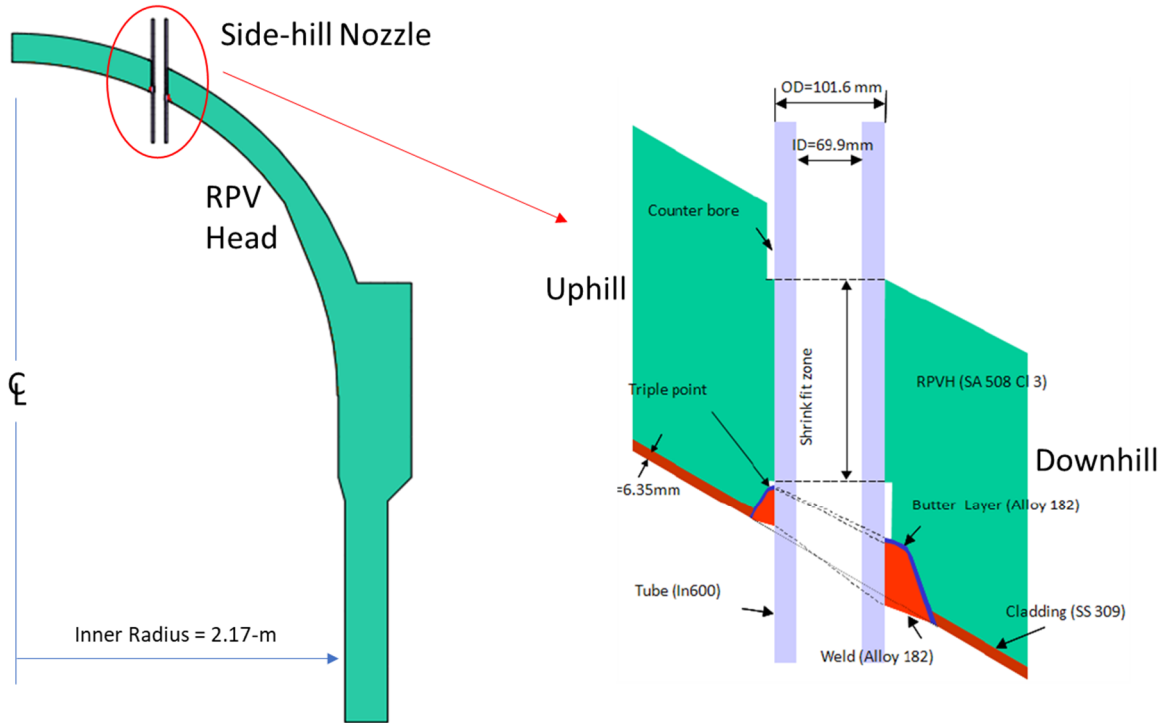


Figure 13 – CRDM Head Segment with Hillside Nozzle Shown with Definitions of Material, Tube and Weld

The methods used to predict the residual stresses due to welding the tube to the head have been fully documented in [9] to [11] and will not be repeated here for brevity. A number of comparisons of the modeling results were conducted with different procedures and with other authors in these papers. The nozzles in a head typically range from the 0° center hole to a maximum angle of near 60°, depending on the PWR manufacturer. In this assessment, the crack growth behavior of a mid-range (25°) nozzle case is studied.

Using a half-symmetric, 22.5° segment FE model, Figure 14 illustrates the Abaqus/Standard FE mesh used to obtain the WRS for this 25° side hillside CRDM tube case. The triple point is illustrated along with the tube (green), the RPV head cladding (blue), and RPV head. As with the other side hill cases discussed in references [9] to [11], the weld was modeled with 14 total passes. The passes were deposited in a ‘quasi’ moving arc fashion where each pass was broken into three sub passes. Each sub pass was deposited as a lump heat input (further details of the method are detailed in [9] to [11]). This approximates the moving arc solution with three segments. This WRS assessment was deemed sufficient and consistent for evaluating the effectiveness of XFEM with the previously reported FEAM assessment of this nozzle [8].

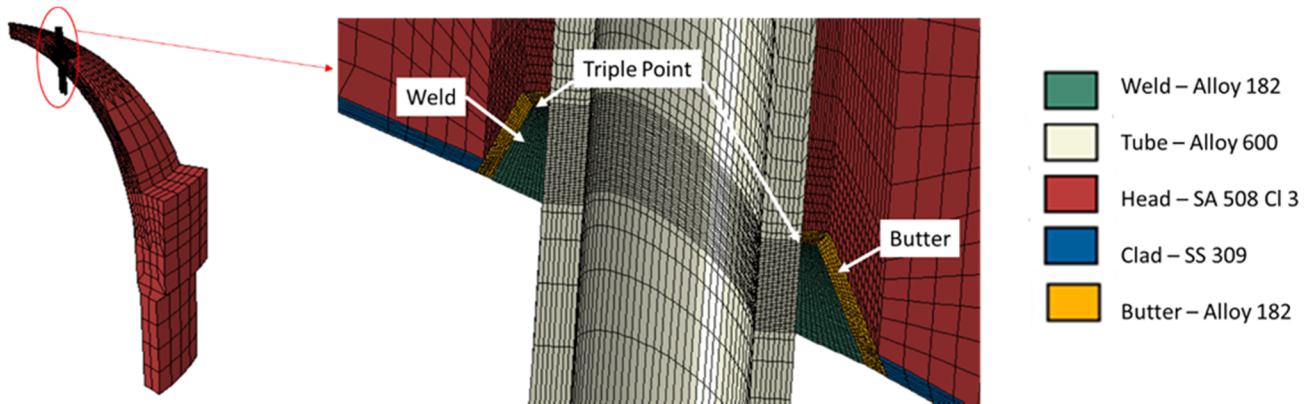


Figure 14 – FE Mesh Used to Generate Hillside CRDM Nozzle Residual Stress Field

The ‘hoop’ direction WRS will drive an axial crack through the J-groove welds. By ‘hoop’ we refer to the tube coordinates in the usual sense. The uphill and downhill hoop WRS is shown in Figure 15. It is seen that the tensile stresses persist not only in the weld but also in the tube. Moreover, the stresses are rather high which is typical of hoop stresses in DMW nozzles. The uphill stresses are higher than the downhill stresses as seen in Figure 15. For a surface crack that is placed at the bottom of the weld, the stress results suggest that the crack will grow faster to the triple point, and incipient leaking in the uphill weld. This initial flaw location assumption is consistent with [8] and was used in this study.

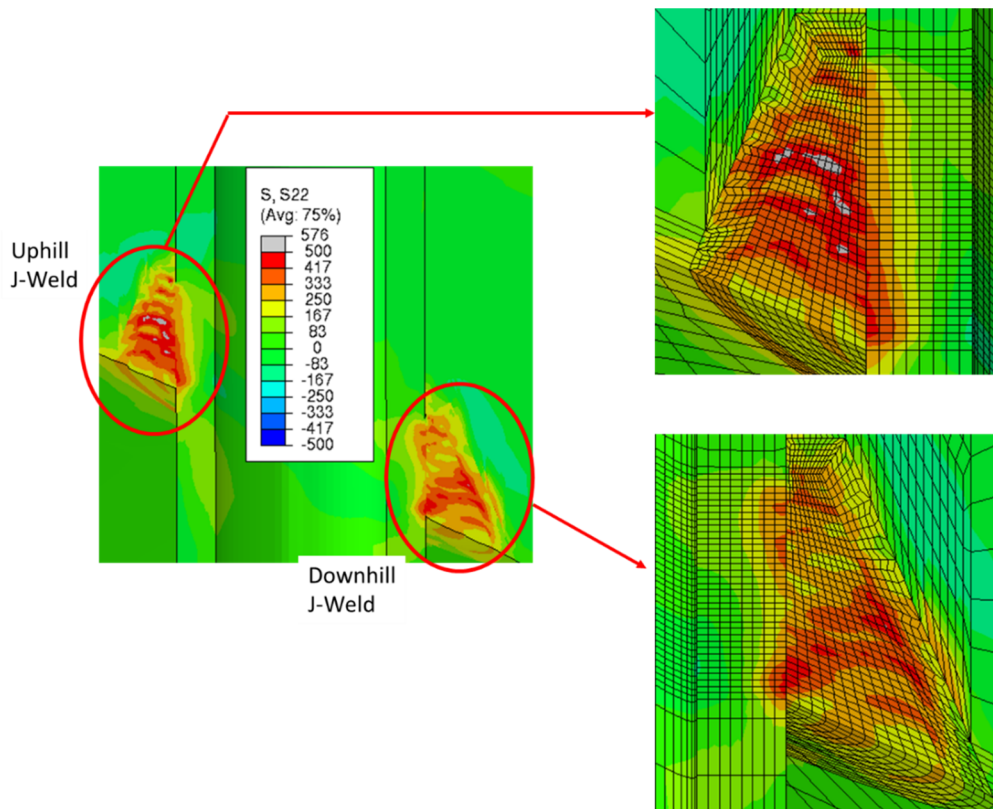


Figure 15 – Hoop Residual Stress Contour Distribution for 25° Hillside CRDM at Room Temperature (20 C) Following Welding and PWHT

Axial crack growth predictions starting in the J-groove weld of an RPV CRDM tube driven by PWSCC was assessed. The XFEM model was used to predict the progressive crack shape as it traversed the weld to the triple point (TP) which represents a breach of the pressure boundary. In order to provide a direct

comparison with the available, bounding FEAM solution [8], an initial semi-elliptical axial surface flaw was located in the Alloy 82/182 on the uphill side of the J-groove weld along the wetted surface for the 25° hillside nozzle.

After the WRS modeling was complete, the WRS FE model was mirrored with the results mapped onto the 45° segment model (see Figure 16) as Abaqus XFEM does not support a symmetry plane and no direct solid geometry was available. The 45° model was imported into Abaqus/CAE where a 10° slice of elements along the uphill section of the 25° nozzle were removed. Geometry was created within this 3D space from which a refined enrichment region, within a 5° slice, was defined.

Finally, the WRS are then mapped onto the modified mesh such that an internal semi-elliptical axial flaw could be propagated using XFEM with PWSCC properties within the Alloy 182 weldment.

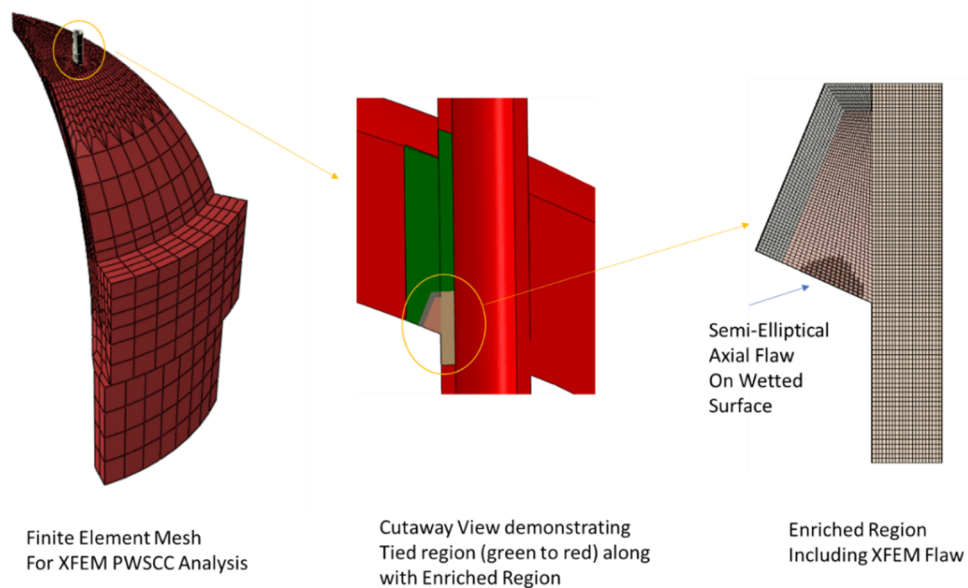


Figure 16 – FE Mesh for the 25° Hillside CRDM PWSCC XFEM Analysis

2.2.2 Modeling Details

Units: N-mm-hour-MPa

FEA Software: Abaqus 2020 (Build ID: 2019_09_13-12.49.31 163176)

Boundary Conditions: Shown in Figure 17, “Plane Sections Remain Plane” constraints were enforced along the A-B-E and C-D-F planes in a cylindrical coordinate system with $u_z = 0$.

Similarly, the A-B-C-D plane was constrained in the global system with $u_y = 0$.

A tie constraint was applied to join the coarse mesh to the 10° refinement mesh which contains the XFEM enrichment region.

A contact pair definition was applied between the tube and the vessel head. No interference fit was modeled. This is consistent with the previous FEAM analysis[8].

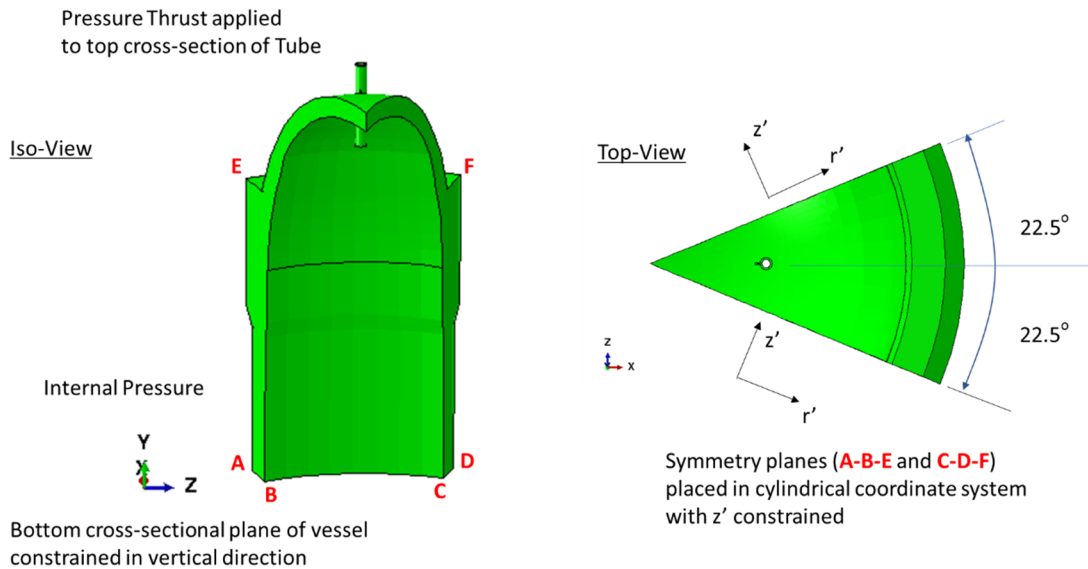


Figure 17 – Key Boundary Conditions and Loadings for the 25° Hillside CRDM PWSCC XFEM FE Model

Loading: The pressure vessel assembly was set to a uniform temperature of 324 °C.

The internal faces of the pipe, including the crack face, was exposed to an internal pressure of 15.5132 MPa (2250 psig).

A corresponding end cap (thrust) loading of $P_y = -13.905$ MPa was applied to the top cross-section of the top of the tube. No piping loads were evaluated.

The residual stress profile (at 323C and including applied pressure) was mapped onto the 45° model via the use of the *MAP SOLUTION capability. Below, the primary driving force hoop stress is shown mapped onto the refined region which contains the XFEM enrichment region.

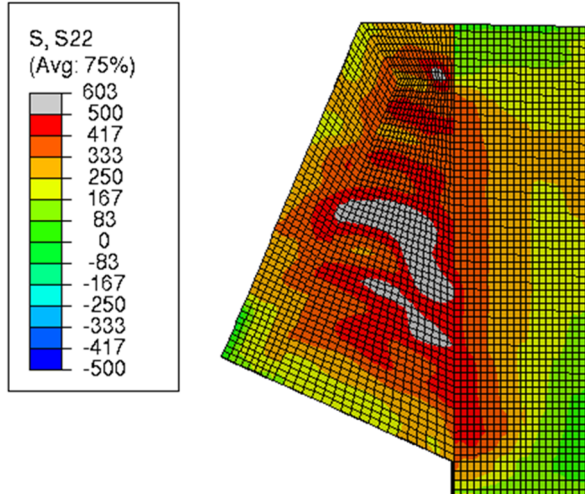


Figure 18 – Initial Residual Hoop Stress Distribution at 324 °C with Internal Pressure included for the 25° Hillside CRDM PWSCC XFEM FE Model (Stress in MPa)

Material: Temperature-dependent Linear Elastic Material Properties were used at 323 °C for the Welded (SMA) Alloy 182, Alloy 600, SS 309, SS 304 and A508 Class 2 materials. All relevant properties are defined and provided within the Supplemental Files Abaqus input files.

For the welded (SMA) Alloy 182 in PWR water conditions which is subject to the PWSCC mechanism, the MRP-115 [7] crack growth rate (75th percentile) for Alloy 182 was adopted in the present study at 324 °C. The temperature of 324C was selected instead of 323 °C to be consistent with the V.C. Summer hot leg DWM assessment.

$$\frac{da}{dt} = 2.0611 \cdot 10^{-3} K^{1.6}$$

when $\frac{da}{dt}$ is in in/year and K is in ksi√in units.

Using the Appendix A Excel tool to convert between unit systems and parameters, the following equation was then used for the strain energy release rate crack growth relation in the required Abaqus format (see Task 2 [2] for more details):

$$\frac{da}{dt} = 4.0516 \cdot 10^{-4} G^{0.8}$$

when $\frac{da}{dt}$ is in mm/hour and G is in N/mm units.

At current, the Abaqus XFEM technology does not have ability to transition between two different materials and, consequently, crack growth rates. As a result, the Alloy 182 crack growth relation was conservatively applied to crack growth in the Alloy 600 tube.

Analysis Steps:

As a precursor to the XFEM assessment, a 22.5° WRS simulation was performed followed by symmetric model generation and results transfer. As these modeling details are of secondary importance for the XFEM assessment, only the necessary restart files are provided in the Supplemental Files. Then, with the use of the *MAP SOLUTION capability, the solution was mapped onto a new 45° 3-D model that contained a 5° slice refined section with the enriched XFEM region with a 4:1 initial XFEM flaw size (2.0-mm deep). *FATIGUE was then used to grow the crack.

The XFEM analysis is completed in two analysis steps:

- 1) *STATIC preload the structure to maximum value.
- 2) *FATIGUE, TYPE=SIMPLIFIED

Elements: 3D first-order 8-node continuum elements were used with the recommended reduced-integration (C3D8R) being the primary choice with full integration (C3D8) being used for a sensitivity analysis.

Meshes: For the baseline assessment, a highly refined structured mesh (0.75-mm x 0.75-mm x 0.75-mm) was utilized within the 5° mesh region that contains the enrichment zone and initial flaw. In the remaining of the model, a 5-mm x 5-mm in-plane mesh was used with 36 elements in the circumferential direction.

Parameters Studied:

The baseline assessment incorporated the Task 2 [2] general recommendations as seen below. The one exception was to incorporate a two order of magnitude increase in the allowable displacement correction (from the default 0.01 to 1.0) for the Newton-Raphson algorithm. In this case, as was discussed in the Task 2 Report Section 3.3.3.2 [2], the XFEM crack propagation analysis failed to converge due to the displacement jump and the sudden increase in local compliance. This relaxation allowed convergence to occur and is not expected to affect the solution accuracy.

Table 5 –Comparison of Task 2 XFEM Modeling Recommendations with the PWSCC CRDM Model

Recommendation Type	Task 2 Recommendations	CRDM Model
Minimum Mesh Refinement: Thickness (crack growth depth direction) Width (crack growth length direction) Height (perpendicular to initial crack plane)	50-elements Use Thickness mesh-seed 10-element with Thickness Mesh Seed	58-elements with 0.75-mm Thickness mesh seed 0.75-mm thickness mesh seed 11-elements with 0.75-mm Thickness mesh seed
Mesh Type:	Structured	Structured
Element Formulation:	Quad/Hex with Reduced Integration	C3D8R (first-order hexahedral with reduced integration)

Shown in Table 6, independent analyses were used to evaluate element formulation, height direction mesh refinement, local element failure control and crack growth damage extrapolation tolerance controls influences on the run times, crack growth rates and shapes as depicted below. The Abaqus CAE model database, input files, and other required files are provided in the Supplemental Materials file.

Table 6 – Summary of Parameters Studied for PWSCC CRDM XFEM Analysis

CRDM Nozzle (25-deg Uphill, Bottom of Weld)	Mesh Refinement		Element Formulation	Mesh Type	Position	Crack Growth			ΔD_{Ntol} Tolerance	Controls Disp Correction	Abaqus Input File Name
	In Crack Plane	Out-of-Plane				RCRACKDIST	NPOLY	ANGLEMAX			
Task 2 Recommendations	Normal	Normal	Reduced	Structured	Default	-	-	-	0.1	1*	CRDM_XFEM_101
Element Formulation											
Full-Integration	Normal	Normal	Full	Structured	Default	-	-	-	0.1	1*	CRDM_XFEM_102
Crack Growth Controls											
*FRACTURE CRITERION, POSITION=											
Nonlocal	Normal	Normal	Reduced	Structured	Nonlocal	Default	Default (7)	Default (85)	0.1	1*	CRDM_XFEM_103
ΔD_{Ntol}					Nonlocal	10	Default	Default	0.1	1*	CRDM_XFEM_104
0.25	Normal	Normal	Reduced	Structured	Default	-	-	-	0.25	1*	CRDM_XFEM_105
			Reduced	Structured	Default	-	-	-	0.01	1*	CRDM_XFEM_113
Mesh Refinement											
OOP Coarse	Normal	Coarse (2x)	Reduced	Structured	Default	-	-	-	0.1	1*	CRDM_XFEM_106
Stationary Crack Study (4mm deep by 10 mm long)											
with WRS and Pressure Loading	Normal	Normal	Reduced	Structured	Default	-	-	-	0.1	1*	CRDM_XFEM_107
XFEM - Full Int	Normal	Normal	Reduced	Structured	Default	-	-	-	0.1	1*	CRDM_XFEM_108
Focused Mesh		Focused	2nd-Order	Structured			N/A		N/A	1*	CRDM_XFEM_109
with Pressure Loading Only	Normal	Normal	Reduced	Structured	Default	-	-	-	0.1	1*	CRDM_XFEM_110
XFEM - Full Int	Normal	Normal	Reduced	Structured	Default	-	-	-	0.1	1*	CRDM_XFEM_111
Focused Mesh		Focused	2nd-Order	Structured			N/A		N/A	1*	CRDM_XFEM_112
Reduced			Reduced								

2.2.3 Benchmark using FEAM

The CRDM uphill J-groove weld axial surface crack evaluation was evaluated using the FEAM methodology results provided by Brust [8].

To introduce the approach, the current FEAM, summarized in references [14, 15], is a state-of-the-art method for obtaining stress intensity factors for three-dimensional surface and embedded crack problems. To conceptualize the technique, the elasticity solution for the union or intersection of two overlapping domains can be found if the solution to each separate problem is known using an iterative process. Since the method is applicable for any number of component geometries, one uses the solution for one infinite domain and one finite domain to obtain the solution to the doubly connected domain represented by the intersection of the two overlaid domains. With the FEAM, the solution for a crack in an infinite solid loaded via arbitrary crack face tractions serves as the infinite domain solution while the finite domain solution is represented by the FE portion of the solution.

Figure 19 schematically illustrates the FEAM method using a simple 2D case for a crack in a weld. The infinite domain solution is actually the complete closed form solution for an elliptic crack in an infinite solid subjected to arbitrary order surface polynomials [16]. The major advantage of the method, as seen in Figure 19, is that a FE mesh of *the uncracked geometry* is all that is needed to obtain stress intensity factors, displacements, stresses, etc. As seen in Figure 19, the solution alternates between the infinite bodies closed form solution and the FE solution for the finite body. Typically, 3 to 4 iterations are required to complete the analyses. The mixed mode stress intensity factors are obtained naturally from this procedure.

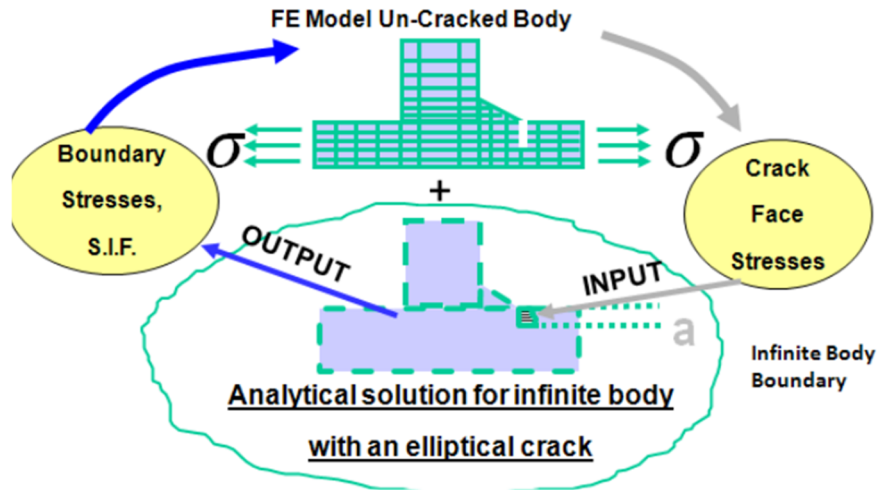


Figure 19 – Illustration of FEAM

The most important aspect of FEAM is that the same mesh can be used to obtain solutions for many different crack sizes, locations, and for multiple cracks. Because the FE stiffness matrix only needs to be reduced once regardless of the crack size, crack location, crack orientation, crack number (mixed mode conditions can be handled as well), etc., the method is extremely computationally efficient. For the K-solutions reported here, solutions of K were obtained within one-minute for the CRDM crack cases studied.

The loads consist of the WRS field (the full field including all six stress components) and pressure loading (including crack face pressure). The analyses were performed by using the following procedure:

1. Perform FEAM analysis with an initial crack (depth, $a = 2$ mm, width, $2c = 8$ mm) as seen at the bottom of the weld in Figure 20 in 'blue'. Note that with the FEAM method, the crack represents the intersection of the ellipse with the mesh and is represented by the shaded region.
2. Extract the stress intensity factors. FEAM obtains the full stress field and calculates the mixed mode values of K (K_I , K_{II} , and K_{III}). For this case, Mode I dominated so that only the Mode I component was used for the PWSCC growth.
3. The stress intensity factors along the crack were extracted and placed in a spreadsheet. K was calculated at 19 locations (every 10-degrees) along the crack. The values of ' K_I ' along the crack front are calculated. Then a crack growth increment is chosen depending on the values of K_I and the crack growth law (above).
4. Only the growth at the deepest point and one at the surface points are used for the next crack size. This was done to be consistent with the axial growth procedure in the tube using the standard influence functions. The crack center was kept identical with the initial location, i.e., it was not moved. For some cracks, the 'ellipse' was rotated after a certain amount of growth if the depth became greater than the width. Note that it would be possible to attempt to fit an 'ellipse' to the best fit around the crack by moving the ellipse center but this was not done here for consistency with the tube growth procedure. This procedure is considered conservative.
5. Go to Step 1 and determine new K values for new crack size. Repeat until crack breaks through the weld.

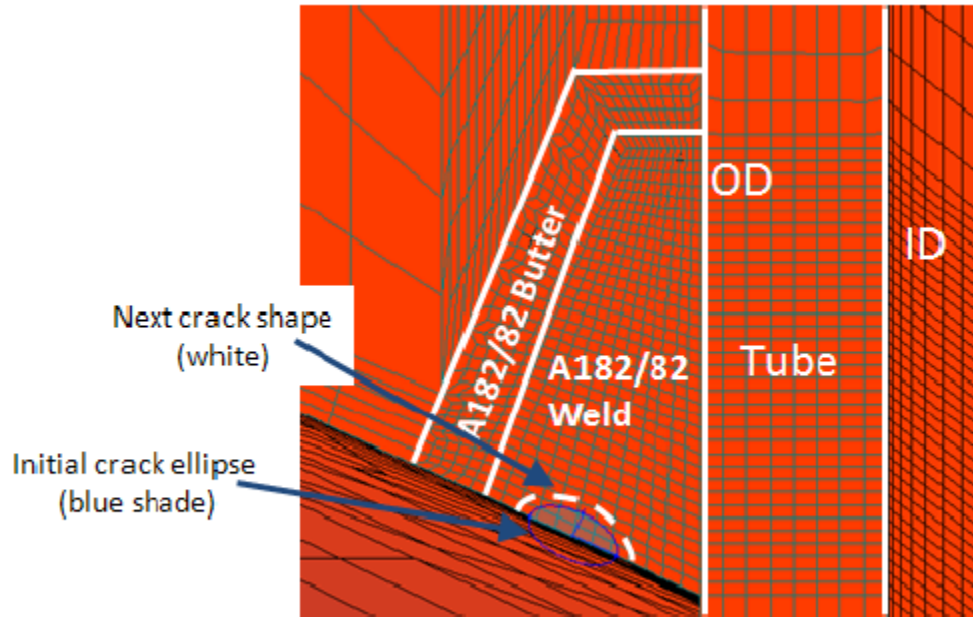


Figure 20 – FEAM Crack Growth Procedures for 25° Hillside CRDM Nozzle Geometry

The FEAM results for the initial 2.0 mm deep by 8.0 mm long axial flaw along the wetted internal surface was grown in ten distinct time points to the TP location. Crack growth rates and shapes will be compared and contrasted to the XFEM solution in Section 2.2.4.7.

2.2.4 Results

2.2.4.1 Comparison of SIF Geometry Correction Factors Between Focused Crack Tip Mesh in Abaqus and Structured Mesh with XFEM Crack Propagation

As there is no known SIF solution for this geometry, a traditional focused mesh geometry model was completed for a 4-mm deep by 10-mm long axial surface flaw on the bottom wetted surface of the Alloy 182 weldment to compare against the XFEM solution. In the focused model seen in Figure 21, a second-order mesh (C3D20R) was used within the highly refined portion of the model with a quarter-point singularity modeled along the semi-elliptical crack front. The built-in Abaqus contour integral capability was used to extract the strain energy release rate (which is equivalent to the J-Integral for the linear elastic solution) for this flaw.

The red-line shown in Figure 21 shows a path from the center of the initial crack extending to the TP. This path will be used to plot crack depth as a function of normalized time to reach the TP. as will be discussed in the results section (2.2.4.2), the time to reach the TP using the POSITION=NONLOCAL analysis was utilized for normalization purposes.

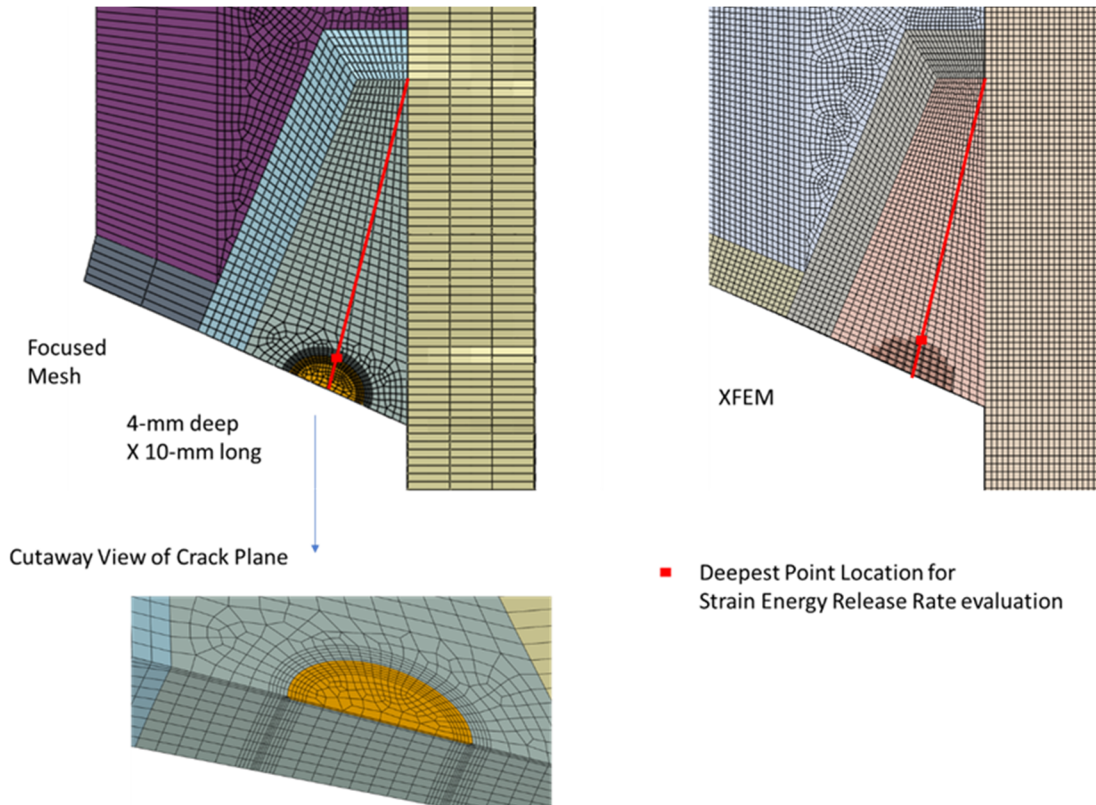


Figure 21 – Location of Strain Energy Release Rate Calculations for Focused and XFEM FE Model Meshes of the 25° Hillside CRDM Nozzle Geometry with a 4-mm by 10-mm Semi-Elliptical Axial Surface Flaw on the Wetted Surface of the J-groove weld

Table 7 compares the focused mesh FEA strain energy release rate solution with results from the full- and reduced integration XFEM baseline models with a normal, structured mesh using the 4-mm deep by 10-mm long semi-elliptical axial flaw size for operating (pressure) loading only and for full WRS and operational loading at 323 °C. In order to compare, the Abaqus XFEM propagating strain energy release variable, ENTRRXFEM, the deepest location of the flaw was selected along the line from the crack initiation point to the TP as defined in Figure 21.

From a results perspective, it can be seen that the internal pressure (including the crack face pressure) contributes approximately 20% of the total driving force. This is consistent with qualitative statements that the WRS is the predominant factor that influences the crack driving force. Similar to the Task 2 3D Flat Plate model [2], the reduced integration CRDM XFEM is seen to better match (10% difference with pressure only and 1% including all loadings) than the full integration case (~15% difference for both loading scenarios). The reduced integration XFEM results are deemed acceptable for this application.

Table 7 – Strain Energy Release Rates at the Deepest Point for the initial 4-mm Deep by 10-mm Long Axial Surface Flaw Along Wetted Surface for the PWSCC CRDM Analysis Comparing Traditional Focused Mesh and XFEM Modeling Techniques (Three-element Average for XFEM Results at a Given Location)

Model Type	Strain Energy Release Rate (N/mm)	
	Pressure Only	Pressure + WRS
Focused Mesh	0.51	2.65
XFEM_Reduced_Integration	0.56	2.70
XFEM_Full_Integration	0.59	3.07

2.2.4.2 Baseline Results

The baseline analysis run (CRDM_XFEM_101) prematurely aborted at 99% normalized time due to a system error associated with the nodal level set calculation as shown in Figure 22. For the analysis to run to completion, the POSITION=NONLOCAL option (CRDM_XFEM_103) was used to smooth the 3D crack front propagation direction. Figure 23 shows the crack depth as a function of normalized time to be essentially equivalent for the two runs. For normalization purposes, the time to reach the TP using the POSITION=NONLOCAL analysis was utilized. For reference, the distance from the center of the initial flaw to the TP is 40.25 mm.

Figure 24 shows the crack shape evolution as a function of normalized time for the PWSCC 25° CRDM axial flaw XFEM assessment. The shape of the XFEM crack growth was driven by the hoop WRS. This is seen in the Figure 24 as the early-stage crack growth is in the depth direction versus the in-plane length. Further, crack growth is first seen to reach the inner tube before the TP. This is in part due to the current Abaqus limitation which precludes different crack growth relations in different materials for the same flaw as the Alloy 600 tube material has a slower crack growth rate than Alloy 182 weldment.

Since the baseline analysis reaches the 99% level, this was still deemed acceptable to produce the desired information following the recommended modeling guidelines.

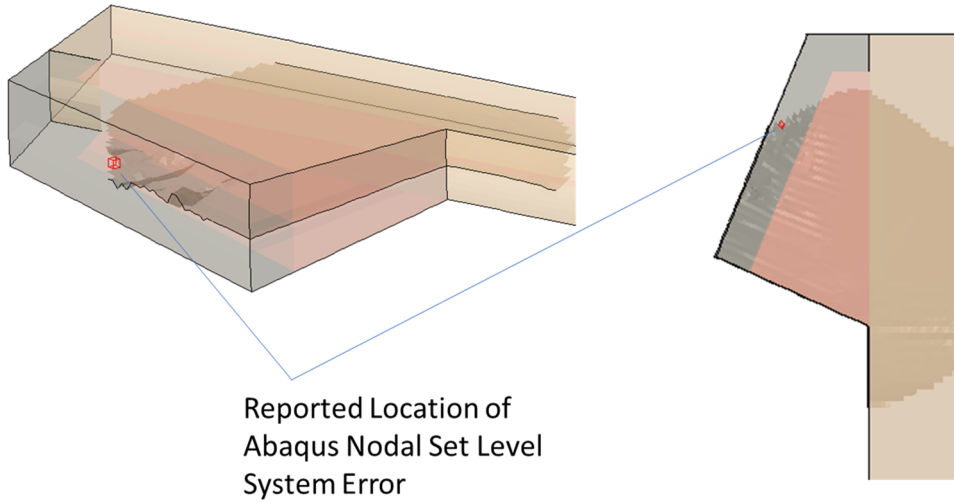


Figure 22 - Crack Shape at 99% TP Growth for the Baseline PWSCC 25° hillside CRDM Axial Surface Flaw Emanating from Uphill Wetted Weldment XFEM FE Model (CRDM_XFEM_101)

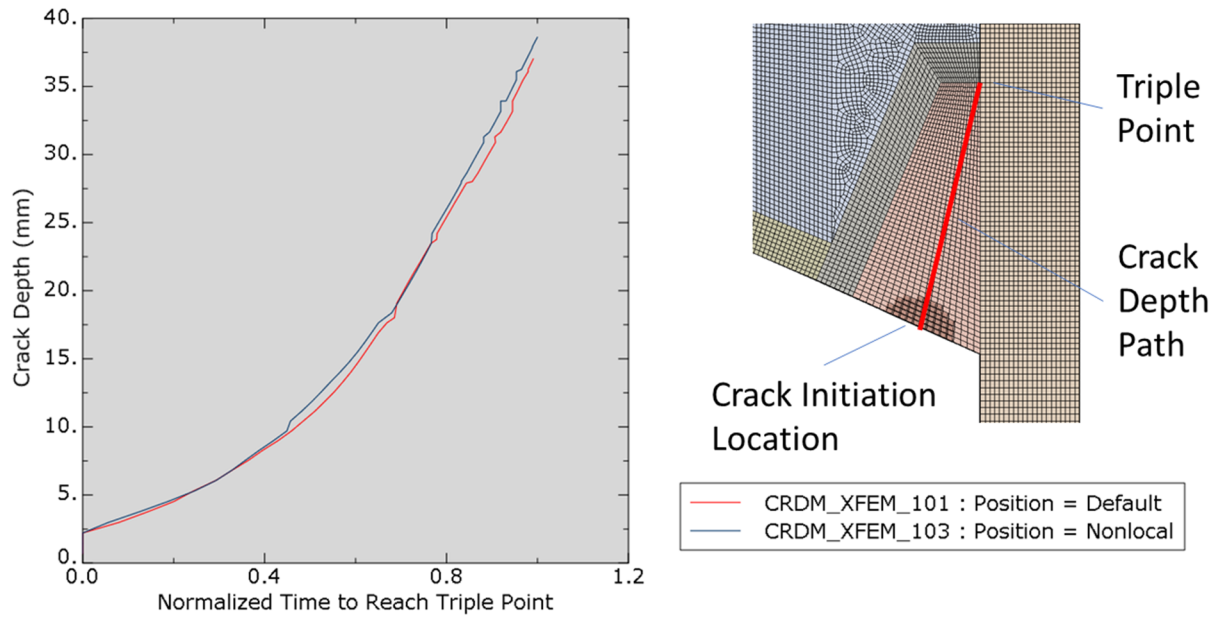


Figure 23 - Crack Growth at Deepest Location for Baseline and PWSCC 25° hillside CRDM Axial Surface Flaw Emanating from Uphill Wetted Weldment XFEM FE Model

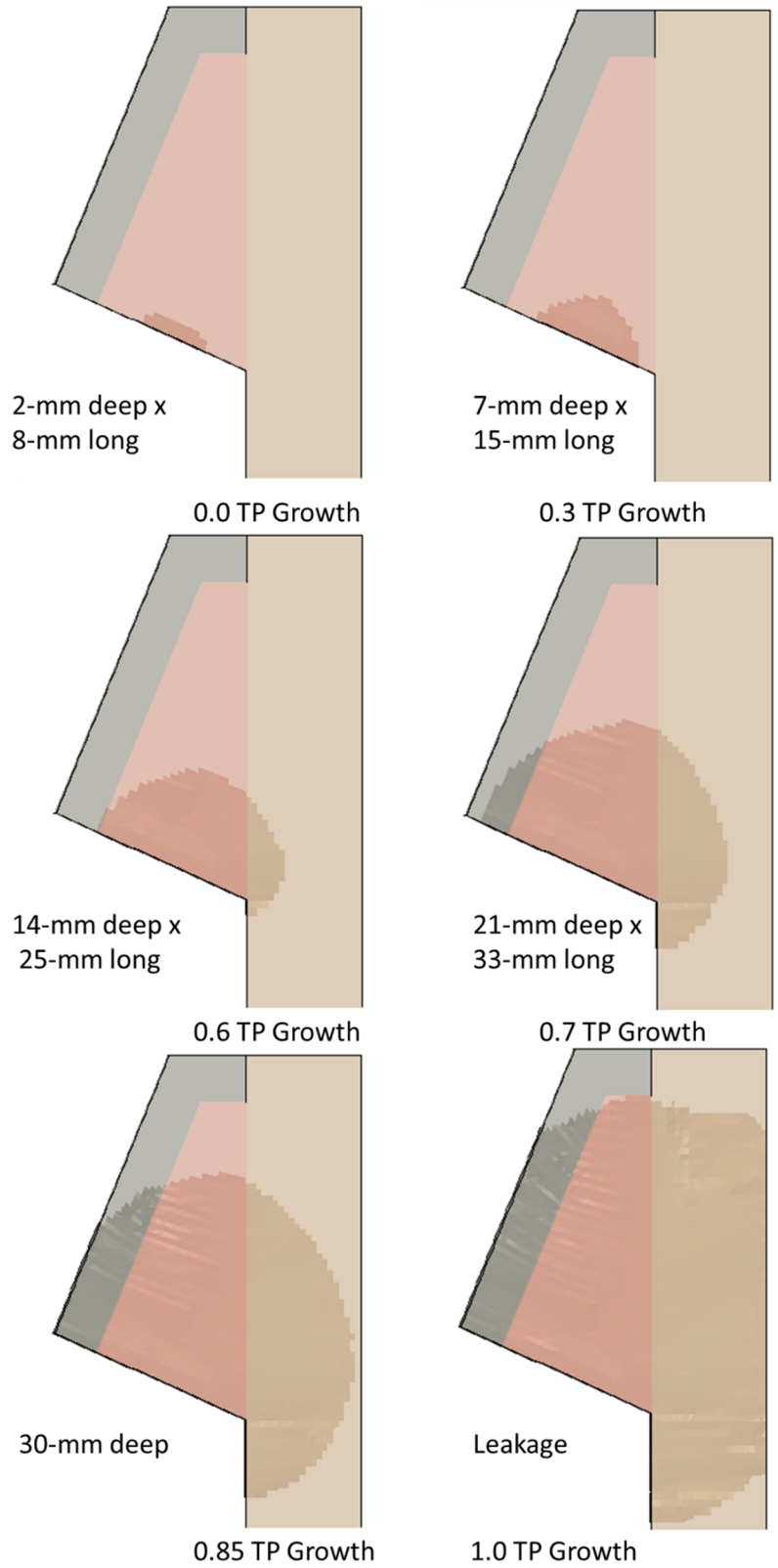


Figure 24 - Crack Shape Evolution as Function of Time for Baseline PWSCC 25° hillside CRDM Axial Surface Flaw Emanating from Uphill Wetted Weldment XFEM FE Model (CRDM_XFEM_101)

2.2.4.3 Influence of Element Formulation Integration

As was indicated in the stationary 4-mm by 10-mm surface flaw SIF sensitivity study, full- and reduced integration solutions were expected to provide similar values during the PWSCC crack growth. Shown in Figure 25, this was true up to the 62% of the TP growth point where a system error occurred for the full integration solution. Since the reduced integration solution was seen to be a closer match for this problem and the other 3D problems reported in Task 2, the reduced integration solution was confirmed to be the preferred recommendation.

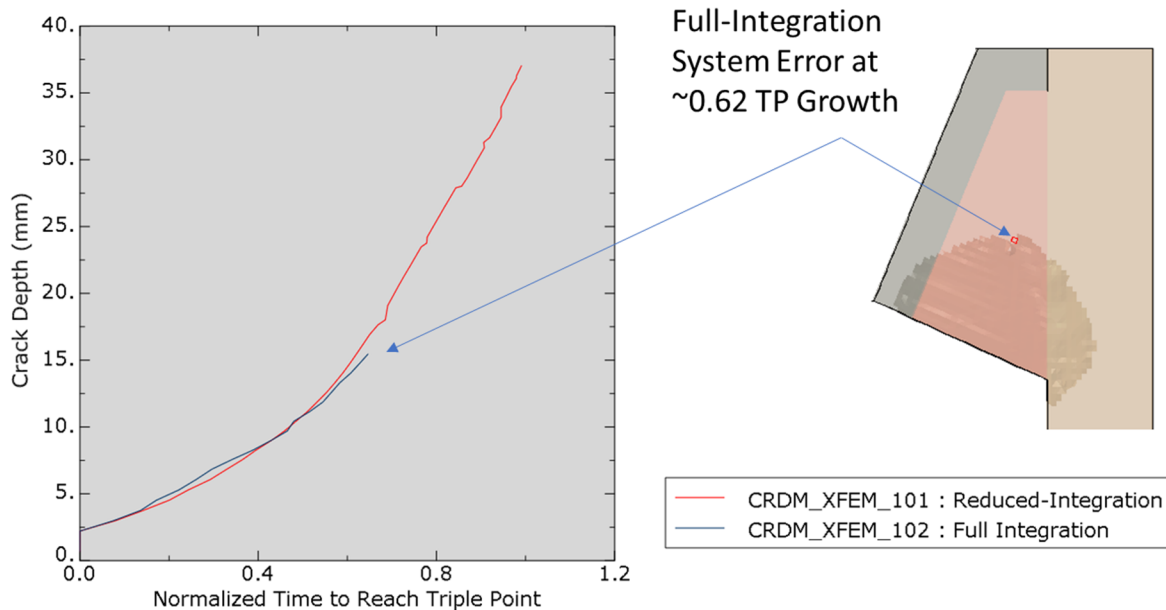


Figure 25 - Crack Growth at Deepest Location for Full- and Reduced Integration PWSCC 25° hillside CRDM Axial Surface Flaw Emanating from Uphill Wetted Weldment XFEM FE Models

2.2.4.4 Local Element Fracture Criterion: Default Versus POSITION=Nonlocal

While it was previously shown that the default usage of POSITION=NONLOCAL with nonlocal stress /strain averaging and crack normal smoothing allowed a converged solution up to the TP, the use of a larger radius around the crack tip was investigated to see if a smoother crack front (less out-of-plane deformation) could be obtained. The *FRACTURE, POSITION=NONLOCAL,RCRACKDIST= parameter was set to a value of 10.0-mm as compared to the default of approximately 3.0-mm (three times the characteristic element length).

Figure 26 shows essentially identical results between the default and 10-mm value run up to the 94% TP Growth where the 10.0-mm parameter is observed to have a system error associate the nodal level set. As a result, the default POSITION=NONLOCAL setting remains the recommendation.

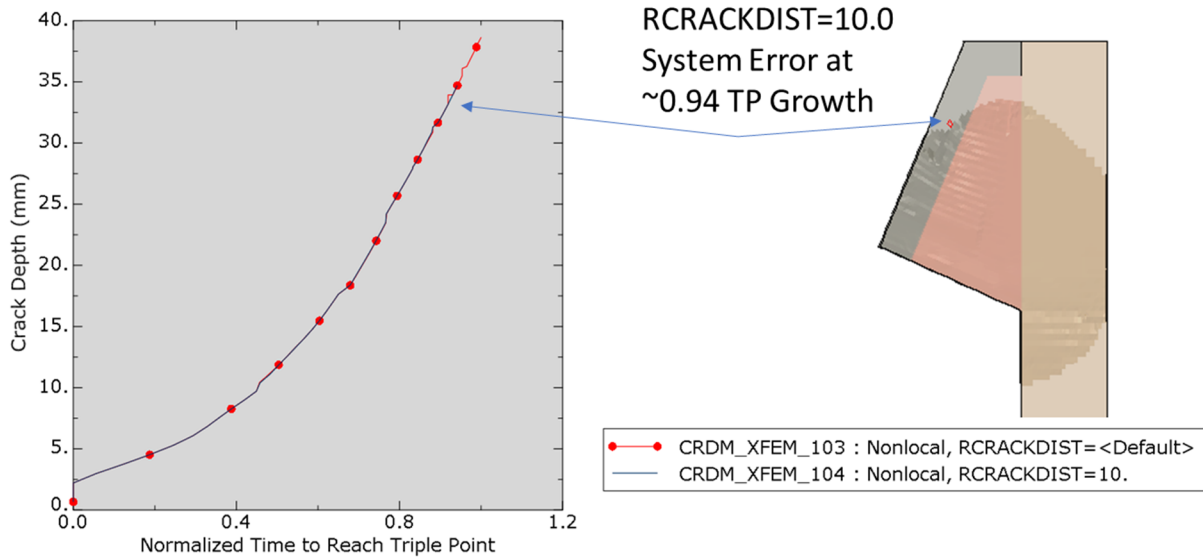


Figure 26 - Crack Growth at Deepest Location for Default and 10.0-mm RCRACKDIST Local Element Fracture Criterion PWSCC 25° hillside CRDM Axial Surface Flaw Emanating from Uphill Wetted Weldment XFEM FE Models

2.2.4.5 Subcritical Damage Extrapolation Tolerance Parameter

For longer running analyses, the damage extrapolation tolerance parameter, ΔD_{Ntol} , can be used to accelerate the subcritical crack growth analysis and to provide a smooth solution for the crack front. Figure 27 shows that increasing ΔD_{Ntol} to 0.25 from the default of 0.1 does increase the crack growth rate. However, Figure 28 does show that the final crack shape at the TP is deviated from the baseline XFEM analysis.

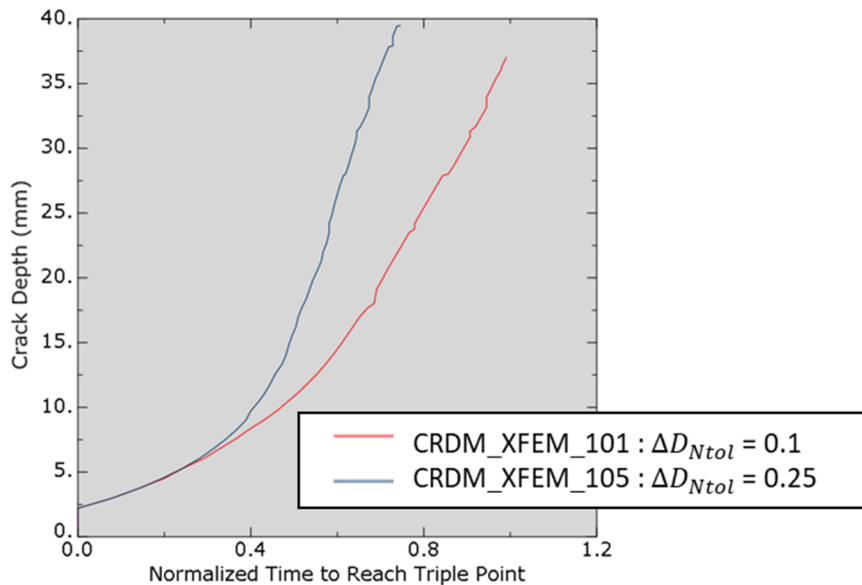


Figure 27 - Crack Growth at Deepest Location for Baseline (0.10) and Increased (0.25) ΔD_{Ntol} PWSCC 25° hillside CRDM Axial Surface Flaw Emanating from Uphill Wetted Weldment XFEM FE Models

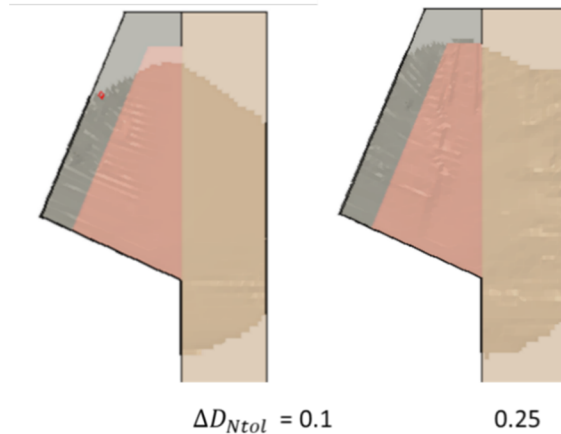


Figure 28 - Crack Shape at TP Depth for Baseline $\Delta D_{Ntol} = 0.10$ and Increased (0.25) PWSCC 25° Hillside CRDM Axial Surface Flaw Emanating from Uphill Wetted Weldment XFEM FE Models

2.2.4.6 Out-of-Plane (Structural Height) Mesh Refinement

As was defined in the Task 2 report[2], the structural height is correlated to a fraction of the structural thickness while still using the structural thickness mesh seed. In so doing, the intent was to create an enriched region mesh with the best formed elements to minimize mesh bias in any direction. To illustrate the value of this recommendation, a sensitivity analysis was made which reduced the number of elements in the structural height direction (out-of-plane to the initial crack plane) from eleven down to five.

Figure 29 shows the coarse mesh refinement along with the crack shape as it interacts with the boundary of the enriched region. It clearly be seen that the crack propagation extension up to the out-of-plane enriched region boundary which is believed to be non-physical.

Further, Figure 30 shows that the crack path trajectory at the deepest point is considerably slower for the coarser mesh. To evaluate further, the strain energy release rate at the initial crack rate was evaluated and found the strain energy release was approximately one-half the value obtained for the baseline analysis. Since the baseline analysis SIF was studied compared to a traditional focused mesh FEA solution earlier in Section 2.2.4.1, the coarser mesh is shown to be unacceptable.

By virtue of the crack shape and crack growth rates, the Task 2 recommendations for mesh refinement were shown to be reasonable and warranted.

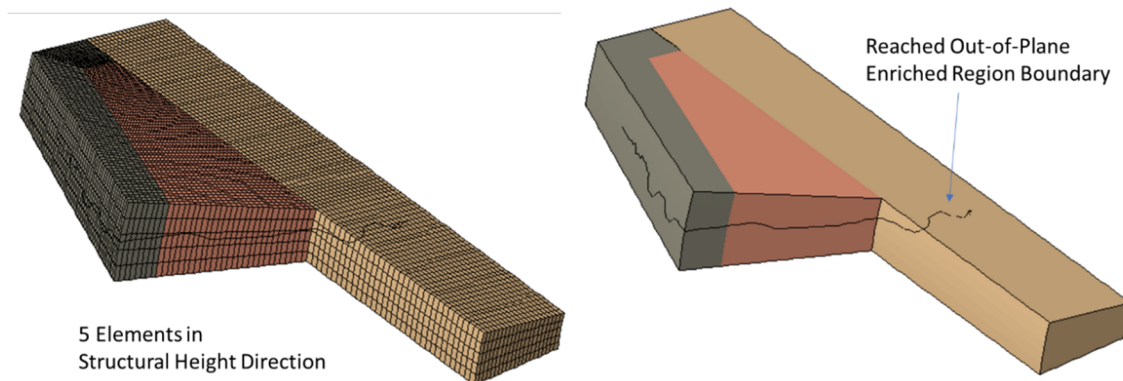


Figure 29 - Crack Growth for Coarse Out-of-Plane PWSCC 25° hillside CRDM Axial Surface Flaw Emanating from Uphill Wetted Weldment XFEM FE Model

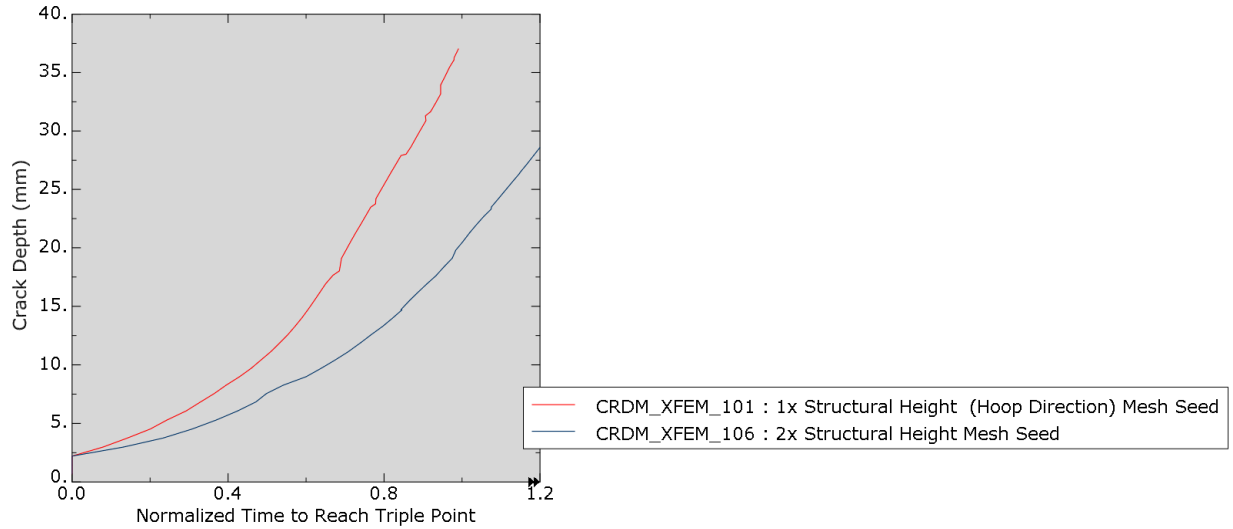


Figure 30 - Crack Growth at Deepest Location for Baseline and Coarse Out-of-Crack Plane Mesh Refinement PWSCC 25° hillside CRDM Axial Surface Flaw Emanating from Uphill Wetted Weldment XFEM FE Models

2.2.4.7 Comparison with FEAM Results

Figure 31 compares the baseline XFEM result with the FEAM results provided by Brust [8]. As seen, a 20% deviation is seen between the approaches in the time required to reach the TP.

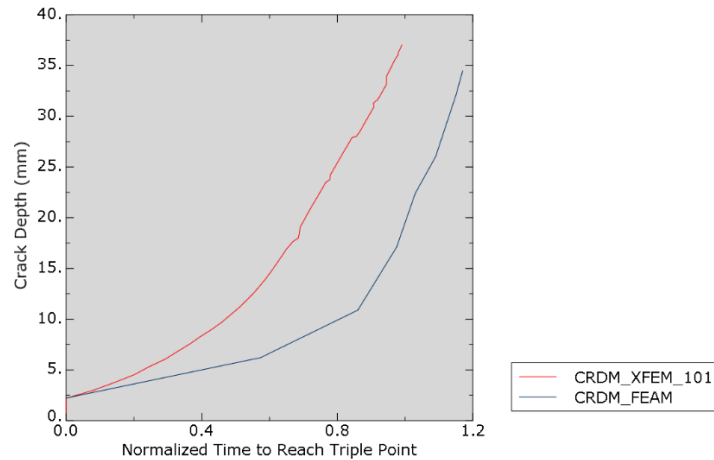


Figure 31 - Crack Growth at Deepest Location for XFEM and FEAM PWSCC 25° hillside CRDM Axial Surface Flaw Emanating from Uphill Wetted Weldment

There are a number of items that could lead to deviations between the two modeling approaches:

- WRS field
Based on Brust [8], the WRS field was replicated in a new Abaqus 2020 analysis based on the available information. While the overall contour trends were correct, it is seen in Figure 32 that the mapped residual stress field does differ spatially and in magnitude, particularly in the tube. Further, the FEAM residual hoop stress magnitudes are actually higher than the corresponding XFEM WRS values which is opposite of the trend expected for the observed crack growth rates.

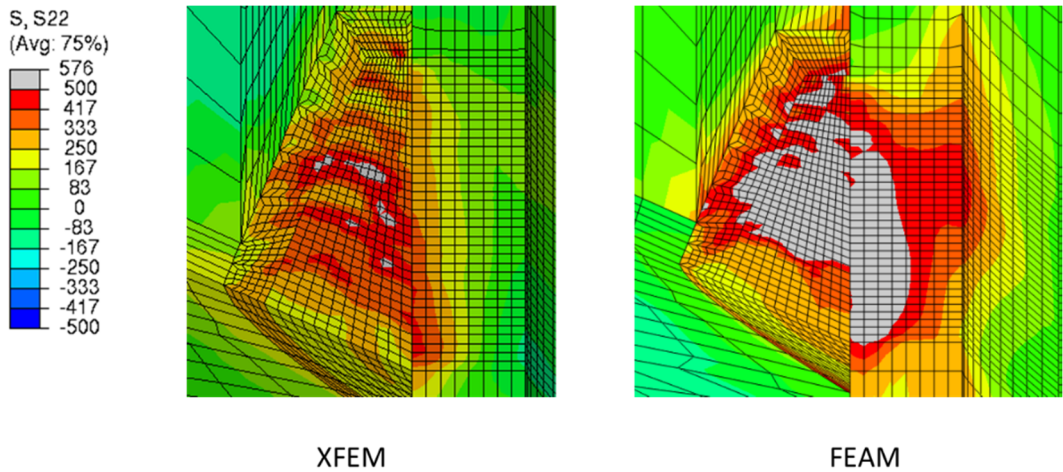


Figure 32 – Welding (Hoop) Residual Stress Contours in MPa for XFEM and FEAM PWSCC 25° Uphill CRDM Weldment Models at 27 °C following Hydrostatic Test. FEAM results taken from [8].

- Strain Energy Release Rate Calculation

As shown earlier within these results, the XFEM strain energy release rate was shown to compare favorably with a traditional focused mesh contour integral extraction using the same WRS and operational loading (pressure and temperature) loadings. However, in comparing Figure 33 (FEAM) with Figure 24 (XFEM), it can be seen that crack length does not reach the tube until the 0.86 TP growth value for the FEAM solution while this occurred at 0.6 TP with XFEM. Further, the XFEM (14.0-mm) has a deeper flaw than the FEAM (10.9-mm) at this crack length (25.0-mm). While this could be associated with the crack shape constraints (elliptical shape) of the FEAM code, additional work would be required to fully identify SIF (or strain energy release rate) differences between these two modeling approaches.

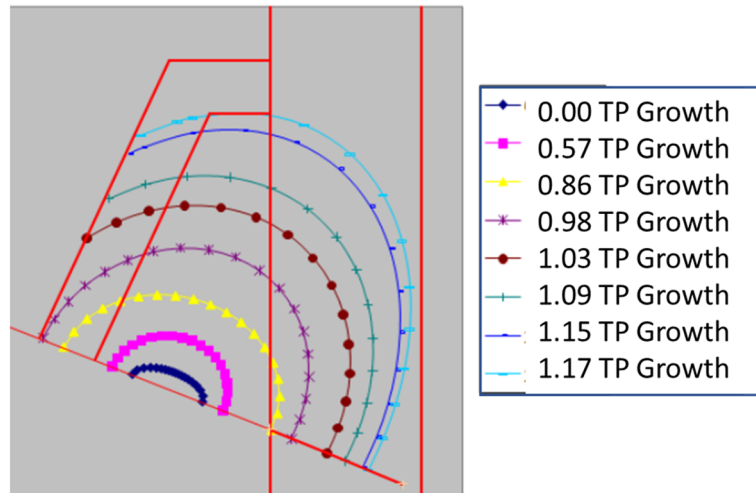


Figure 33 – Crack Shape Evolution as Function of Time for PWSCC 25° hillside CRDM Axial Surface Flaw Emanating from Uphill Wetted Weldment FEAM Model [8]

- Subcritical Damage Extrapolation Tolerance Parameter

It has been previously discussed that the default (0.10) subcritical crack growth tolerance parameter, ΔD_{Ntol} , should provide a conservative solution for a given assessment. Figure 34 compares a tighter tolerance value of 0.01 with the default 0.10 along with the FEAM solution. It is shown that the 0.01 solution is still conservative as compared to the FEAM solution.

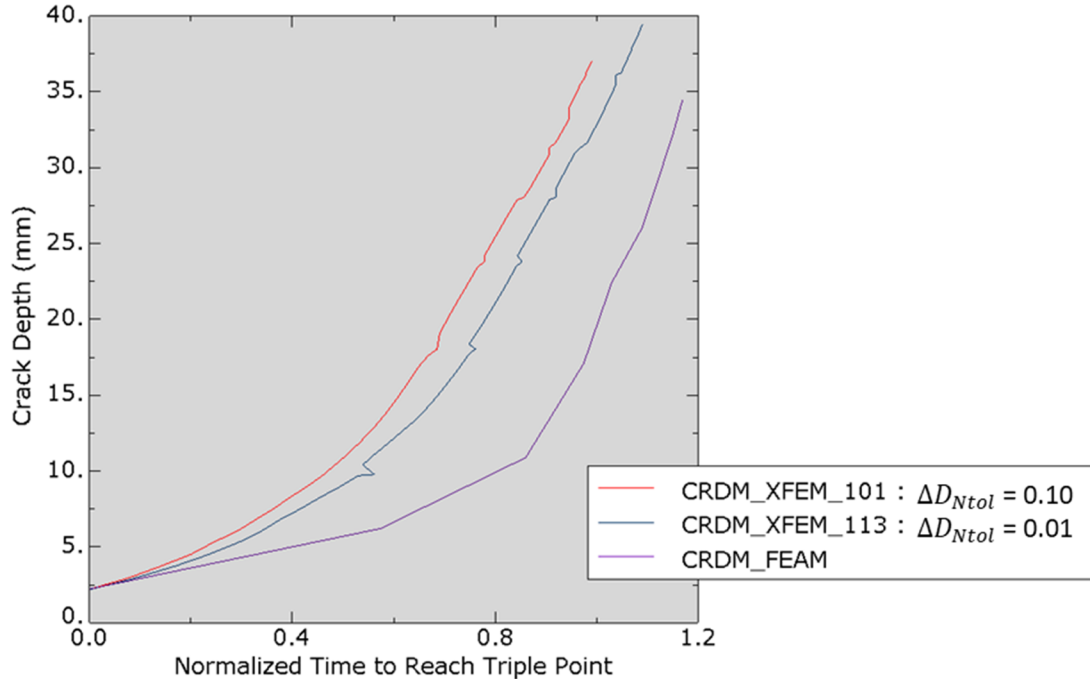


Figure 34 - Crack Growth at Deepest Location for Baseline (0.1) and Tight (0.01) Subcritical Damage Extrapolation Tolerance Parameter XFEM Solutions Compared to the FEAM Solution for the PWSCC 25° hillside CRDM Axial Surface Flaw Emanating from Uphill Wetted Weldment

2.2.4.8 Computational Resources

In terms of computational cost, the self-contained built-in Abaqus XFEM analyses are expensive but viable runs. Shown in Table 8, the baseline analysis using 10-cores on a Dell PowerEdge T640 server with a 20-core Intel® Xeon® Gold 6148 chip at 2.4 GHz with sufficient memory to keep all calculations in core takes slightly over 2 days. The only parameter that significantly changes solution time is variation of the subcritical damage tolerance parameter, ΔD_{Ntol} . By increasing the ΔD_{Ntol} to 0.25, the runtime is reduced by approximately 6x while ensuring that a more conservative crack growth rate is obtained. This may be of benefit when a rough estimate, but not necessarily the most accurate, solution is required. Conversely, the decreasing of ΔD_{Ntol} to 0.01 increases the run time by 40% with increased crack front accuracy.

Table 8 – Computational Resources for the PWSCC V.C. Summer Axial Surface Flaw in DWM Hot Leg XFEM for Different Fracture Criteria and Crack Growth Control Parameters

	CRDM_25deg		
	Analysis Run:	101	105
ΔD_{Ntol} :	0.1	0.25	0.01
Computer Wallclock Time * (hrs)	51.8	8.0	71.0
Increments	3201	497	4386
Iterations	3201	497	4386

* All computer runs were made with 10 cores on a 20-core Intel® Xeon® Gold 6148 at 2.4 GHz

2.2.5 Summary

Using the general XFEM modeling recommendations defined in the Introduction section, the built-in Abaqus XFEM capability has shown to be capable of modeling planar crack growth for relatively complex PWSCC CRDM model applications in terms of crack growth rate and crack shape metrics.

While using essentially the same linear elastic modeling assumptions associated with crack growth, the XFEM approach was found to be approximately 20% more conservative in terms of crack depth growth rate than the previously modeled assessment using FEAM. There are a number of differences between the two approaches (WRS profile, assumed crack shape, SIF solution extraction, etc.) which have been identified which contribute to the differences. Still, for the current study, the observed differences are deemed to be acceptable.

Model stability (robustness) is an issue with the current release of Abaqus associated with the nodal level set calculation for the growing crack. As tabulated below, 50% of the sensitivity runs completed in this CRDM study resulted in a system error (code abort). Limited crack path oscillatory behavior was observed in these problems. As a result, the built-in Abaqus XFEM capability for this application should be viewed as a research rather than production tool.

Table 9 – Summary of Key Parameters and Analysis Result for PWSCC CRDM Crack Growth Analyses

CRDM Nozzle	Mesh Refinement		Element Formulation	Crack Growth		ΔD_{Ntol} Tolerance	Abaqus Input File Name	Analysis Result	% Triple Point
	In Crack Plane	Out-of-Plane		Position	RCRACKDIST				
Task 2 Recommendations	Normal	Normal	Reduced	Default	-	0.1	CRDM_25deg_101	Code Abort	98.1%
Element Formulation	Normal	Normal	Full	Default	-	0.1	CRDM_25deg_102	Code Abort	71.4%
Crack Growth Controls									
*FRACTURE CRITERION, POSITION=	Normal	Normal	Reduced	Nonlocal	Default	0.1	CRDM_25deg_103	Triple Point	100.0%
				Nonlocal	10	0.1	CRDM_25deg_104	Code Abort	93.8%
ΔD_{Ntol}	Normal	Normal	Reduced	Default	-	0.25	CRDM_25deg_105	Triple Point	100.0%
			Reduced	Default	-	0.01	CRDM_25deg_113	Triple Point	108.9%

3 KEY OBSERVATIONS

3.1 Quality of Results

- Using the general XFEM modeling recommendations, the built-in Abaqus XFEM capability was shown to be capable of modeling planar crack growth for these relatively complex PWSCC applications in terms of crack growth rate and crack shape metrics.
- The built-in Abaqus XFEM was found to be within 20% of crack growth rates and similar crack growth shapes when compared to the previously reported assessments using the natural crack growth approach (DMW nozzle) and the FEAM (CRDM nozzle). When the differences in modeling assumptions between the various approaches are considered, this is believed to be quite reasonable.
- To improve the quality of simulation, the built-in Abaqus XFEM capability will need an enhancement to include the ability to handle different crack growth rates between materials (e.g. crack growth from Alloy 82 J-groove weld into the Alloy 600 tube). At current, this capability is not available in the built-in version or via the UMIXMODEFATIGUE user subroutine.
- In previous PWSCC assessments, the actual fracture analysis involving the natural crack growth method and FEAM assume that the material properties are linear elastic. For consistency, the XFEM assessments maintains this assumption. However, it is appreciated that the materials are in fact elastic-plastic with residual stresses near or at the yield surface. As the crack propagates, redistribution will occur that would be different than the linear elastic assumption. This effect should be investigated in the future.

3.2 Stability of Solution

- There has been seen a model stability (robustness) issue with the current release of Abaqus associated with the nodal level set calculation for growing cracks in relatively complex problems.
 - Approximately 50% of the sensitivity runs completed in the CRDM study and in the V.C. Summer DMW nozzle assessments resulted in a system error (code abort).
 - In the code abort message, the level set is reported to be essentially perpendicular to the existing crack plane.
 - The code abort location is predominately but not exclusively along the crack front adjacent to the enriched region boundary.
 - There appears to some amount of crack path oscillatory behavior even in analysis cases that run to completion; however, more pronounced oscillations are seen to more likely result in code aborts.
 - At no time prior to the code abort are any Newton-Raphson convergence problems noted in the solution.
- Due to the model stability issue, the built-in Abaqus XFEM capability for this application should be viewed as a research rather than production tool.
 - For the current Abaqus capability, there does not appear to be a systematic set of modeling parameters that consistently precludes this from occurring.
 - The modeling recommendations defined in Task 2 and summarized in the Introduction remain the most stable parameters to provide accurate solutions.

3.3 Computational Resources

- Due to the high degree of parallelization of the Abaqus XFEM implementation, solutions can be obtained in reasonable time periods even for these relatively complex analyses. Still, these relatively complex crack growth analyses can be expected to utilize high computational resources as simulations can range from 36 to 72 wall clock hours using 10 to 20 computational cores on high-end workstations.
- Using non-default values for subcritical damage extrapolation tolerance parameter ΔD_{Ntol} option of greater than 0.1, solutions can be obtained in a shorter amount of time, but some accuracy loss can be seen in the crack shape while the crack growth rate will be conservative.
- In relation to other numerical techniques, such as the linear elastic natural crack growth approach and the FEAM, those solutions will be faster from a processor time perspective (on the order of a dozen solver passes). However, unless proper scripting algorithms exist, the setup time will likely reduce the total analysis time advantage.

4 CONCLUSIONS

Using the general XFEM modeling recommendations, the built-in Abaqus XFEM capability was shown to be capable of modeling planar crack growth for these relatively complex PWSCC applications in terms of crack growth rate and crack shape metrics.

After successful comparison of the strain energy release rate for the initial flaw size with published fitness-for-service solutions, the V.C. Summer hot leg DWM nozzle flaw was grown from the internal wetted surface to the outer diameter of the Inconel 182 weldment. In so doing, the final crack shape was found to qualitatively match with the post-mortem through-wall axial flaw. Crack growth rates were found to be within 2% when compared to a natural crack growth flaw analysis.

Similarly, for the hillside CRDM nozzle, the strain energy release rate was compared between the XFEM propagating crack strain energy release rate and a traditional focused mesh contour integral extraction of the strain energy release rate for the initial flaw size. XFEM results were found to be match within 10%. With this confidence, PWSCC crack growth was performed from this internal wetted surface of the weld to the TP (tube-weld-head) which represents a pressure boundary breach. While using essentially the same linear elastic modeling assumptions associated with crack growth, the XFEM approach was found to be approximately 20% more conservative in terms of crack depth growth rate than the previously modeled assessment that used the FEAM.

To summarize, the XFEM assessments were found to be within 20% of crack growth rates and similar crack growth shapes when compared to the previously reported assessments using the natural crack growth approach (DMW nozzle) and the FEAM (CRDM nozzle). When the differences in modeling assumptions between the various approaches are considered, this is believed to be quite reasonable

Still for this capability, solution stability remains a concern which may require sensitivity runs to obtain a solution to the desired crack size. As a result, the built-in Abaqus XFEM capability for this application should be viewed as a research rather than production tool.

In this current study, we have limited our study to planar extension for pre-existing axial flaws. The subsequent Task 4 report provides a summary of solutions performed by the NRC and contractors, and other organizations that may be used in the future for further benchmarking. The benchmark solutions presented provide references along with other data necessary to perform XFEM based solutions and predicted results using other PWSCC growth methods for benchmark comparisons. In particular, future PWSCC studies can include damage initiation into a macrocrack (per [4]) and circumferential flaw DMW nozzle evaluations (per [12]).

REFERENCES

- 1) Dassault Systèmes (2020), *Abaqus/Standard 2020 User's Manual*, Providence, RI, USA.
- 2) Hill, L.T., Brust, F.W. and Kalyanam, S. (2020), "Support for XFEM Component Integrity: Task 2 Sensitivity Study of PWSCC-type Crack Growth in Abaqus XFEM," Submitted to U.S. Nuclear Regulatory Commission as part of Prime Contract NRC-HQ-25-14-E-0004 Task Order 31310019F0075, Draft 6/19/2020.
- 3) Hwang, S. S. (2013), "Review of PWSCC and mitigation Management Strategies of Alloy 600 materials of PWRs," *Journal of Nuclear Materials*, Vol. 443, pp. 321-330.
- 4) Lee, S-J and Yoon-Suk, °C. (2015), "Crack Initiation and Growth Simulation for CRDM Nozzles by Extended Finite Element Method," 2015 ASME Pressure Vessels and Piping Division Conference, Boston, MA, USA.
- 5) Scott, P. et al. (2005), "The Battelle Integrity of Nuclear Piping (BINP) Program Final Report," Volumes 1 and 2, NUREG/CR-6837, US Nuclear Regulatory Commission, Washington, D.C., USA.
- 6) Shim, D.-J., Kalyanam, S., Punch, E., Zhang, T., Brust, F., Wilkowski, G., Goodfellow, A., and Smith, M. (2010), "Advanced Finite Element Analysis (AFEA) Evaluation for Circumferential and Axial PWSCC Defects," PVP2010-25162, 2010 ASME Pressure Vessels and Piping Conference, Bellevue, WA, USA.
- 7) Materials Reliability Program (2004), "Crack Growth Rates for Evaluating Primary Water Stress Corrosion Cracking (PWSCC) of Alloy 82, 182, and 132 Welds," MRP-115, EPRI, Palo Alto, CA, USA.
- 8) Brust, F.W., Zhang, T., Shim, D.-J., Wilkowski, G. and Rudland, D. (2011), "Modeling Crack Growth in Weld Residual Stress Fields using the Finite Element Alternating Method," 2011 ASME Pressure Vessels and Piping Division Conference, Baltimore, MD, USA.
- 9) Rudland, D., Chen, Y., Zhang, T., Wilkowski, G., Broussard, J. and White, G. (2007), "Comparison of Welding Residual Stress Solutions for Control Rod Drive Mechanism Nozzles," 2007 ASME Pressure Vessels and Piping Division Conference, San Antonio, TX, USA.
- 10) Rudland, D., Zhang, T., Wilkowski, G. and Csontos, A. (2008), "Welding Residual Stress Solutions for Dissimilar Metal Surge Line Nozzles Welds," 2008 ASME Pressure Vessels and Piping Division Conference, Chicago, IL, USA.
- 11) Chen, Y., Rudland, D., and Wilkowski, G. (2004), "Impact of Welding Sequence on the CRDM Nozzle-to-Vessel Weld Stress Analysis," 2004 ASME Pressure Vessels and Piping Conference, San Diego, CA, USA.
- 12) Shi, Y., Duan X. and Wang, M. (2019), "Modeling of Natural Crack Growth with XFEM," 25th International Conference on Structural Mechanics in Reactor Technology 2019 (SMiRT 25), Charlotte, NC, USA.

- 13) API 579-1/ASME FFS-1 (2016), Fitness for Service, American Petroleum Institute, Washington, DC, USA.
- 14) Nishioka, T. And Atluri, S. N. (1983), "Analytical Solutions for Embedded Elliptical Cracks, and Finite Element Alternating Method for Elliptical Surface Cracks, Subjected to Arbitrary Loadings," Engineering Fracture Mechanics, Vol 17, pp. 247-268.
- 15) Stonesifer, R. B., Brust, F. W., and Leis, B. N. (1993), "Mixed-Mode Stress Intensity Factors for Interacting Semi-Elliptical Surface Cracks in a Plate," Engineering Fracture Mechanics, Vol. 45, pp. 357-380.
- 16) Vijayakumar, K., and Atluri, S. N. (1981), "An Embedded Elliptical Crack, in an Infinite Solid, Subject to Arbitrary Crack-Face Traction's," Journal of Applied Mechanics, Vol 103, pp. 88-96.
- 17) Miranda, A.C.O., Meggiolaro, M.A., Castro, J.T.P., Martha, L.F. and Bittencourt, T.N. (2003), "Fatigue life and crack path predictions in generic 2D structural components," Engineering Fracture Mechanics, Vol. 70, pp. 1259-1279.
- 18) ASME Boiler and Pressure Vessel Code Cases – Nuclear Components (2019), Code Case N-770-5 "Alternative Examination Requirements and Acceptance Standards for Class 1 PWR Piping and Vessel Nozzle Butt Welds Fabricated With UNS N06082 or UNS W86182 Weld Filler Material With or Without Application of Listed Mitigation Activities Section XI, Division 1", New York, NY, USA.
- 19) Alexandreanu, B., Chopra, O.K. and Shack, W.J. (2008), Crack Growth Rates and Metallographic Examinations of Alloy 600 and Alloy 82/182 from Field Components and Laboratory Materials Tested in PWR Environments, NUREG/CR-6964, US Nuclear Regulatory Commission, Washington, DC, USA.
- 20) Shim, D.-J., Uddin, M., Kalyanam, S., Brust, F.W. and Young, B. (2015), "Application of Extended Finite Element Method (XFEM) to Stress Intensity Factor Calculations," PVP2015-45032, ASME 2015 Pressure Vessels and Piping Conference, Boston, MA, USA.
- 21) González–Albuixech, V.F., Giner, E., Tarancón, J.E., Fuenmayor F.J., and Gravouil, A. (2013), "Domain integral formulation for 3-D curved and non-planar cracks with the extended finite element method," Computer Methods in Applied Mechanics and Engineering, Vol. 264, pp. 129-144.

APPENDIX A – PARAMETER AND UNIT CONVERSION EXCEL TOOL

Provided in the Supplemental Files is a unit and parameter conversion tool for driving force (K-to-G and G-to-K) and Paris Law (ΔK -to- ΔG and ΔG -to- ΔK) coefficients. This tool can be used for cycle-dependent (i.e. fatigue) and time-dependent (e.g. PWSCC) Paris-like crack growth relations.

For this capability, we have coded a Visual Basic macro within Excel. Step-by-Step instructions are provided within the spreadsheet. This tool can be used as a standalone spreadsheet or embedded within a website. Please note that there are limited error checks in place to trap data input errors.

As an example for the crack growth relation, we can review the Miranda [17] work where the SAE 1020 fatigue constants were given in the same general form as:

$$\frac{da}{dN} = 4.5 \cdot 10^{-10} \Delta K^{2.1}$$

with $\frac{da}{dN}$ in m/cycle and ΔK in $MPa\sqrt{m}$.

Going through the necessary plain-strain conversion for a pure N-m unit system, the Paris Law-like ΔG relation required by Abaqus becomes:

$$\frac{da}{dN} = 9.1685 \cdot 10^{-11} \Delta G^{1.05}$$

with $\frac{da}{dN}$ in m/cycle and ΔG in $\frac{N}{m}$.

Elastic Properties			Stress State	
Young's	Units	ν	Plane Stress Plane Strain	
2.00E+05	Pa MPa GPa	0.3		

da/dN Units	Paris Law		
	C Value	Units	n
input	4.5000E-10	MPa·mm ksi·in GPa·mm	2.10
output	1.1303E-22	Pa·m MPa·mm MPa·in	2.10

Paris Law		
C Value	Units	n
9.1685E-11	N/mm N/in lbf/in	1.05
9.1685E-11	N/mm N/in lbf/in	1.05

Step 1. Enter crack growth rate units
 Step 2. Enter Young's modulus and units
 Step 3. Enter ν
 Step 4. Select stress state
 Step 5. Enter the crack growth exponent, n
 Step 5. Enter input/output units for ΔK and ΔG
 Step 6. Enter C input value for ΔK or ΔG
 Step 7. Press Calculate Paris Law Coefficients

Calculate Paris Law Coefficients

In an analogous manner, the fracture driving force (or toughness) can be converted between common units of K and G. Shown below, a fracture toughness of $K=100 MPa\sqrt{m}$ is converted to $K=91.0 ksi\sqrt{in}$, $G=4.55E4 N/m$ and $G=259.81 lbf/in$.

Elastic Properties			Stress State	
Young's	Units	ν	Plane Stress Plane Strain	
2.00E+05	Pa MPa GPa	0.3		

Fracture Toughness					
K Value	K		G Value	G or J	
	Units			Units	
1.0000E+02	Pa·m MPa·mm MPa·in		4.5500E+04	N/mm N/in lbf/in	
9.1005E+01	GPa·m psi·in ksi·in		2.5981E+02	N/mm N/in lbf/in	

Step 1. Enter Young's modulus and units
 Step 2. Enter ν
 Step 3. Select stress state
 Step 4. Enter input/output units for K and G
 Step 5. Enter input value for K or G
 Step 6. Press Calculate Fracture Toughness

Calculate Fracture Toughness